

# KSC VAB Aeroacoustic Hazard Assessment

Justin M. Oliveira<sup>1</sup>, Sabrina Yedo<sup>2</sup>, and Michael D. Campbell<sup>3</sup>  
*NASA, Kennedy Space Center, FL, 32899*

Joseph P. Atkinson<sup>4</sup>  
*ASRC Aerospace Corporation, Titusville, FL, 32780*

NASA Kennedy Space Center (KSC) carried out an analysis of the effects of aeroacoustics produced by stationary solid rocket motors in processing areas at KSC. In the current paper, attention is directed toward the acoustic effects of a motor burning within the Vehicle Assembly Building (VAB). The analysis was carried out with support from ASRC Aerospace who modeled transmission effects into surrounding facilities. Calculations were done using semi-analytical models for both aeroacoustics and transmission. From the results it was concluded that acoustic hazards in proximity to the source of ignition and plume can be severe; acoustic hazards in the far-field are significantly lower.

## Nomenclature

$A$	area, m <sup>2</sup>
$A_w$	A-weighted sound pressure level correction, dB
$a$	speed of sound, m/s
$b$	line support spacing, m
$C$	model coefficient
$c$	phase velocity, m/s
$d$	diameter, m or interior wall spacing, m
$DI$	directivity index, dB
$F$	thrust or force, N
$f$	frequency, Hz
$L$	length, m
$L_w$	overall sound pressure level, dB
$M$	Mach number
$m$	mass per unit area, kg/m <sup>2</sup>
$\dot{m}$	mass flow rate, kg/s
$OASPL$	overall sound pressure level, dB
$P, p$	pressure or overpressure, Pa
$R$	gas constant, J/kg-K or distance to receiver from plume source, m
$R_A$	A-weighted frequency sensitivity weighting function, W

<sup>1</sup> Lead Analyst, Analysis Branch, Kennedy Space Center, FL.

<sup>2</sup> Safety Engineer, Safety Engineering & Assurance Branch, Kennedy Space Center, FL.

<sup>3</sup> Division Chief, S&MA Integration Division, Kennedy Space Center, FL.

<sup>4</sup> Mechanical Engineer, Structures Analysis Branch, Titusville, FL.

$S$	total absorption surface area, $m^2$
$S_n$	Strouhal Number
$SPL$	sound pressure level, dB
$s$	plume path length from nozzle to source, m
$T$	temperature, K
$TL$	transmission loss, dB
$t, a$	thickness, m
$V$	velocity, m/s
$W$	sound power, W or weight, lb
$w, h$	width, m
$W_{OA}$	overall acoustic sound power, W
$x_t$	plume core length, m
$\alpha$	absorption coefficient
$\beta$	geometric angle from receiver to local plume slice flow direction, radians
$\beta_{eff}$	effective angle corrected for Strouhal Number effects, radians
$\Delta f$	bandwidth of frequency band, Hz
$\Delta x_t$	plume slice length, m
$\eta$	acoustic efficiency, decimal or wall/window-panel material loss factor
$\gamma$	specific heat ratio
$\lambda$	wavelength, m
$\nu$	Poisson's Ratio
$\rho$	density, $kg/m^3$
$\sigma$	modulus of elasticity, psi
$\theta$	incidence angle, radians
$\tau$	transmissivity

#### Subscripts

$amb$	ambient
$b$	point b
$B, 0$	nozzle/bore
$c$	chamber or critical
$d$	point d
$e$	nozzle exit or point e
$f$	frequency or point f
$i$	incident
$p$	outer sheet of sandwich
$ps$	plume slice
$ps, f$	plume slice, frequency
$r$	reflected
$tot$	total
$0$	nozzle/bore, blast-origin, or fundamental
$1$	lower critical
$2$	higher critical
$*$	sonic condition

## I. Introduction

THE Vehicle Assembly Building (VAB) was built to allow processing of Apollo Program launch vehicles in the 1960's and later was adapted to process the Space Shuttle launch vehicles. Since then the VAB has served effectively as the location to assemble and mate solid rocket boosters (SRB) to the vehicles External Tank (ET) and Orbiter. The VAB will again be adapted to process new human and non-human rated launch vehicles in support of NASA's strategic plan for space exploration.

Previously, for the Space Shuttle Program (SSP), the Kennedy Space Center (KSC) Safety Office determined a safe separation distance (SSD) of 1,315 feet for the inhabited building distance (IBD) [7]. The calculation used the Department of Defense (DoD) explosive safety standards (sometimes referred to as the weight based approach). The SSP safe separation distance for the VAB, derived using the DoD weight based approach, allows for processing of up to four complete Shuttle SRB's containing approximately 4.44 million pounds of solid propellant. The currently proposed Constellation Program (CxP) launch schedule could require assembly and storage of nearly 13 million pounds of hazard classification 1.3 propellants; up to eight 5-segment ARES-V boosters to be stored in the VAB simultaneously. Using the weight based approach for eight ARES-V boosters would result in a safe separation distance of 1,810 ft. This distance extends beyond a number of high occupancy facilities in the area around the VAB. The NESC concluded that the DoD weight based approach was overly conservative for SRMs with a 1.3 hazard classification. NASA Engineering and Safety Center (NESC) recommended that an alternative approach based on calculating the threat due to each hazard component (heat flux, toxics, acoustics, etc.) be pursued [1].

In the event of an inadvertent ignition, several hazardous components could either prevent or restrict egress of personnel and potentially impact the surrounding facilities. A methodology development as well as an assessment of the noise levels in proximity of the VAB was required to support the alternative approach recommended by the NESC. Acoustic SSD's as well as levels of resistance nearby facilities have from acoustic energy was addressed. Several scenarios were considered and later in the study the case set was bounded using results from parallel studies. These parallel studies helped narrow the VAB building configuration and ignition propagation as a result of an inadvertent ignition. The emphasis of this study was placed on the far-field sound hazards to personnel and the effectiveness of surrounding facilities as safe heavens from acoustic energy.

Prediction of aero-acoustic noise as well as transmission into nearby facilities was performed using semi-analytical models. The facilities modeled were those in immediate proximity to the VAB; the Launch Control Center (LCC) and Orbiter Processing Facility #3 (OPF-3). An exposure criterion for personnel was developed to establish safe separation distances. All methodologies and findings were examined by a NASA peer review committee.

## II. Modeling Assumptions

Currently, CxP would reuse the VAB with minor modifications to support processing of the Ares-I/V vehicles. The VAB is the fourth largest building in the world by volume. It consists of 4 High Bays used to process NASA launch vehicles, each assembled on a Mobile Launch Platform (MLP). Several platform levels are used to perform processing operations and will too be reused and/or modified. Each HB is separated by concrete walls (lightly reinforced) and large steel columns which provide the main support to the structure.

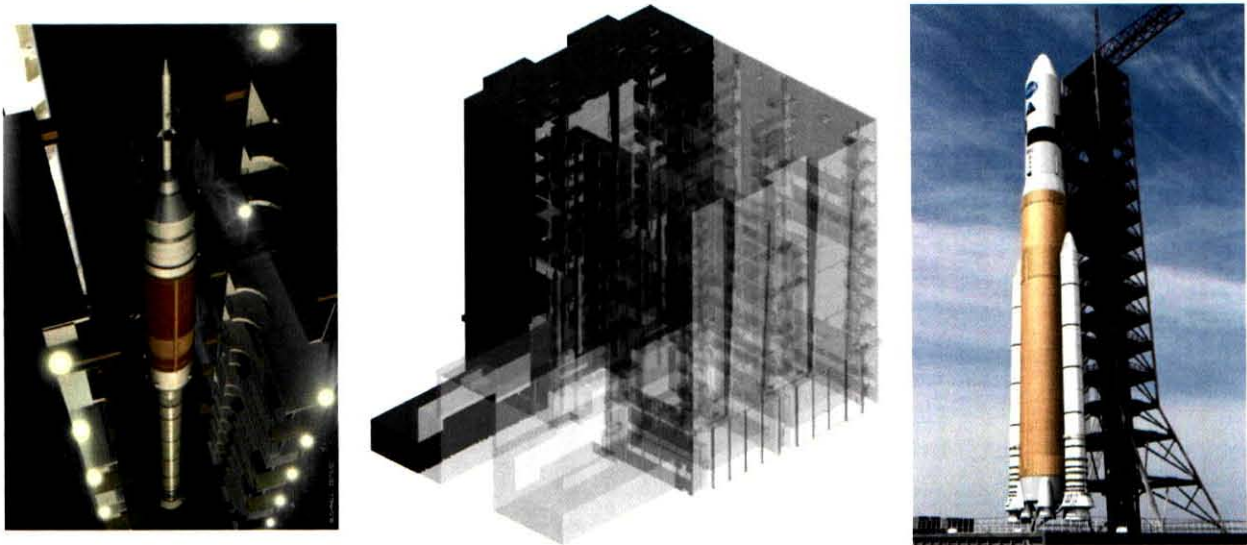


**Figure 1:** *NASA Ares-I/V Flight Vehicles and the VAB*

The shell is made up of hundreds of aluminum “punch-out” panels which are designed to fail above approximately 100 psf (meant to protect the facility from large pressure loading during severe weather). It was shown from CFD models that the pressure loading from ignition over-pressure (IOP) and plume impingement (resulting from an inadvertent ignition) would knock over internal walls and fail all VAB paneling. In summary, shortly after ignition only the VAB ceiling, main supports, and ML’s would remain intact; it was assumed the vehicles remain intact. This assertion was used in the acoustic modeling and helped to simplify the analysis such to make the acoustic fields diffuse into a fourth space.

Though a fully processed vehicle would certainly become propulsive if an inadvertent ignition occurred, an uncapped booster would not. This is because the chamber pressure isn’t sufficient enough to create enough thrust. To simplify the analysis, it was assumed that all burning boosters were fixed in place in the VAB. Furthermore nozzle gimbling and motor pitching was ignored.

Furthermore it was assumed that plumes emanating from boosters and impinging on the VAB floor/ceiling spread symmetrically. This assumption made the acoustic calculations easier because the fields could be treated as two-dimensional. Also, in scenarios where adjacent boosters (on the same MLP) burned together (and in the same direction), their plume acoustic powers were combined and an equivalent plume was computed. This simplification is typically done in aeroacoustics since the plumes become conjoined if in close proximity.

Sound absorption (dissipation) from the atmosphere is dependent on temperature and relative humidity. The atmosphere at KSC is fairly humid year round (typically 40-95%) and temperature can vary between extremes (typically 35-105° F). Above approximately 4 kHz, temperature and relative humidity become competing effects.

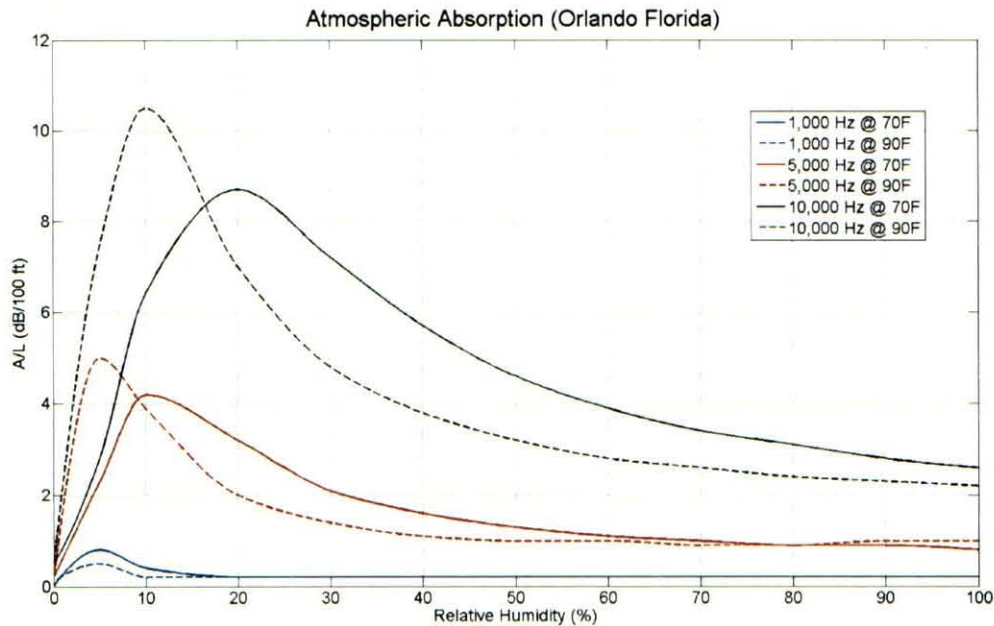


**Figure 2:** Atmospheric Sound Absorption versus Relative Humidity (for various frequencies and temperatures)

The dissipation from atmospheric absorption can be significant above 5 kHz. For this study the absorption was ignored to be conservative and simplify the analysis. Furthermore, ground reflections other than the initial plume deflection were ignored.

### III. Theoretical Background

The computational modeling of aeroacoustics from plumes is difficult because of the small time steps and large flow times required to resolve spectra (10 kHz  $\sim 10^{-4}$  seconds). Furthermore, models used to convert the unsteady-

turbulent fields to acoustic sources are computationally expensive. Alternatively, semi-empirical methods have been used that combine theoretical equations with empirical correlations. The method used in this study breaks the plume into several slices which are converted to monopole sources (see figure below).

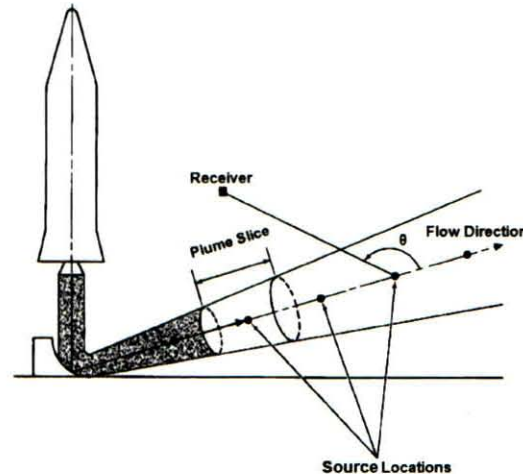


**Figure 3:** *Plume conversion into acoustic sources* [2]

The sources are then characterized and sound is radiated inside the domain. This method has proven to give good agreement with measured data. Most recent, comparisons with data from the Ares-IX launch showed phenomenal agreement (see a summary below).

Proximity	Spectrum Error	OASPL Error
Near-field; ML/Launch Pad (0-500')	± 0.5 dB	+ 1 dB
Mid-field; Launch Site (1000-1400')		
Far-field; adjacent pad/VAB (5000-10,000')	± 5 dB	

**Figure 4:** *Model error determined from Ares-IX launch test data*

#### IV. Exposure Criteria

Several sources stating the sound pressure levels associated with human exposure exist. OSHA standard 1019.95 [3] provides exposure limits for industrial areas based on exposure time. Because capped and uncapped boosters can burn for long periods of time (> 5 minutes), using the OSHA table would result in a 115 dBA exposure limit. The intent of the OSHA table was for use in industrial environments and not for inadvertent ignition-type events. Furthermore, use of the OSHA value would result in a large SSD (overly conservative). Hearing damage will largely affect a person's ability to egress because of the ear's sensitivity.

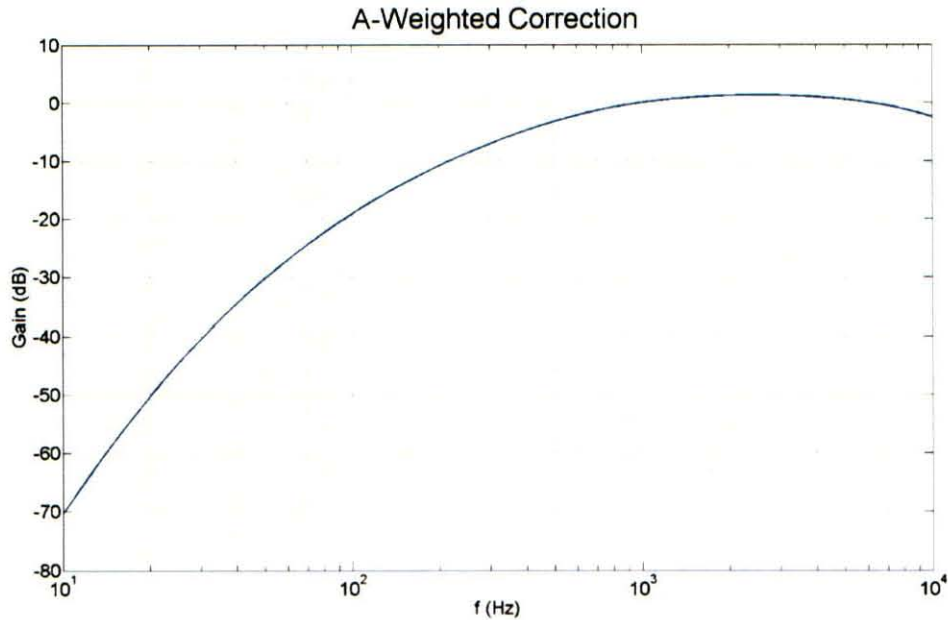


**Figure 5:** *A-Weighted Correction* [4]

Ruptured ear drum(s) will impede a person's balance and ability to egress; this occurs around 160 dB [4]. The ear's threshold of pain occurs around 140 dB; intense nausea is typical at levels around and above 158 dB [4].

The personnel exposure limit used in this study was 140 dB (corresponding to the threshold of pain). At these levels personnel will experience a large degree of permanent and irreversible hearing damage but not ear drum rupture; thus allowing the ability to egress. Because of the  $\log(R^2)$  nature of acoustic sound propagation, revising the criteria upward will drastically reduce the SSD. Also, OASPL levels are measured at a head level of 5'6" and revision of this target height to a larger value would also drastically reduce the SSD.

## V. Calculation Methodology

Acoustic predictions were performed using a modified Eldred's 2nd Method. The plume is broken into several slices and given a unique spectrum. The sound pressure from all the slices (at each octave band frequency) is summed to determine the net sound pressure at a specific point. This is done first by solving for the plume metrics using the chamber conditions. Using provided chamber conditions and nozzle geometry, nozzle exit conditions were found assuming 1D compressible isentropic flow [6]. Assuming the flow to be choked at the nozzle throat, mass flow rate is found,

$$\dot{m} = \frac{p_c A^*}{\sqrt{T_c}} \sqrt{\frac{\gamma_c}{R_c} \left( \frac{2}{\gamma_c + 1} \right)^{(\gamma_c+1)/(\gamma_c-1)}} \quad \text{Eq. 1}$$

The exit Mach number is found using the area-Mach number relation,

$$\left( \frac{A_e}{A^*} \right)^2 = \frac{1}{M_e^2} \left[ \frac{2}{\gamma_c + 1} \left( 1 + \frac{\gamma_c - 1}{2} M_e^2 \right) \right]^{(\gamma_c+1)/(\gamma_c-1)} \quad \text{Eq. 2}$$

The equation has two solutions; subsonic and supersonic condition. Since the chamber pressure is such that it's above the critical pressure ratio, we assume the supersonic solution.

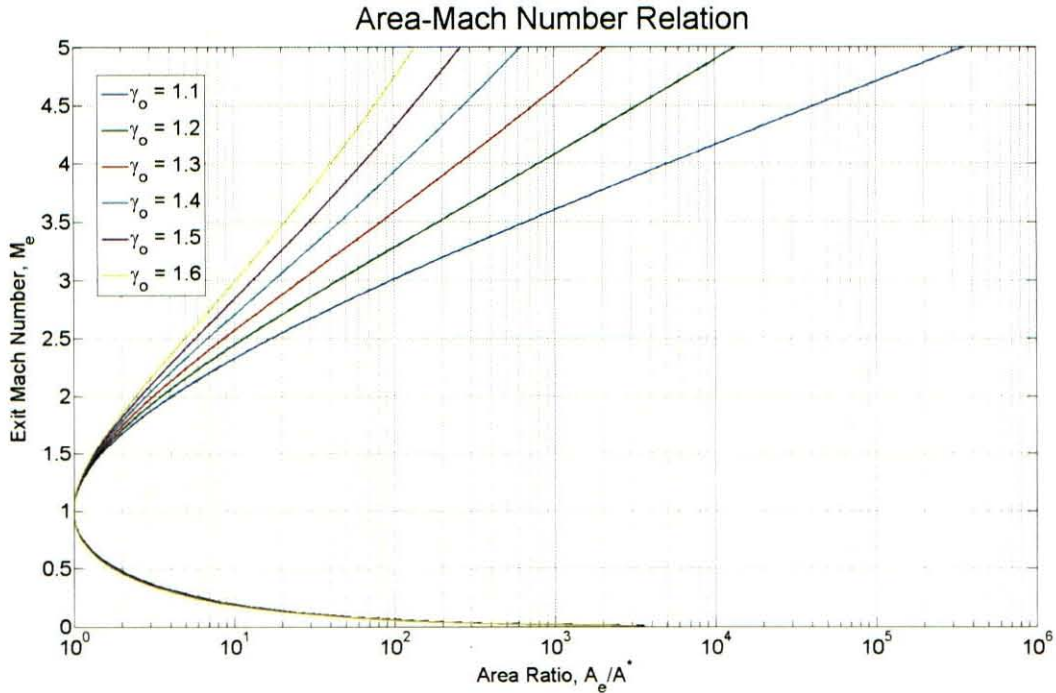


**Figure 6:** Area-Mach number relation (for various specific heat ratios)

The exit plane pressure is then found using the Mach number,

$$P_e = P_c \left( 1 + \frac{\gamma_c - 1}{2} M_e^2 \right)^{-\gamma_c/(\gamma_c-1)} \quad \text{Eq. 3}$$

Knowing the exit Mach number, the exit plane temperature is then found,

$$T_e = T_c \left( 1 + \frac{\gamma_c - 1}{2} M_e^2 \right)^{-1} \quad \text{Eq. 4}$$

With the exit temperature found, exit plane speed of sound is found,

$$a_e = \sqrt{\gamma_c R_c T_e} \quad \text{Eq. 5}$$

The exit plane velocity is found then using the Mach number and speed of sound,



$$V_e = M_e a_e \quad \text{Eq. 6}$$

Thrust is then found to be [9],

$$F = \dot{m}V_e + (P_e - P_{amb})A_e \quad \text{Eq. 7}$$

Plume core length is found using the exit Mach number-diameter correlation [2],

$$\frac{x_t}{d_e} = 3.45(1 + 0.38M_e)^2 \quad \text{Eq. 8}$$

This correlation was derived from various experimental data sets of various plume types; it was a least-square-type fit to that data.

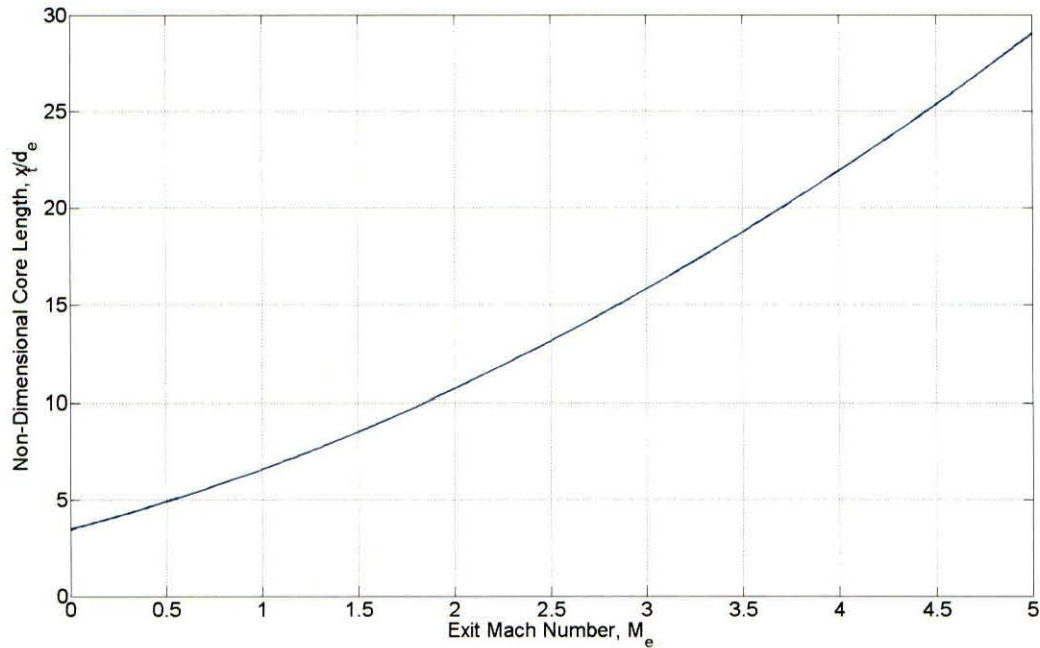


**Figure 7:** *Non-dimensional plume core length*

In order to calculate the overall sound power, an acoustic efficiency must be used. With direct floor impingement, the efficiency is found using the data in SP-8072 in conjunction with the nozzle geometry and placement relative to the VAB floor and/or ceiling.

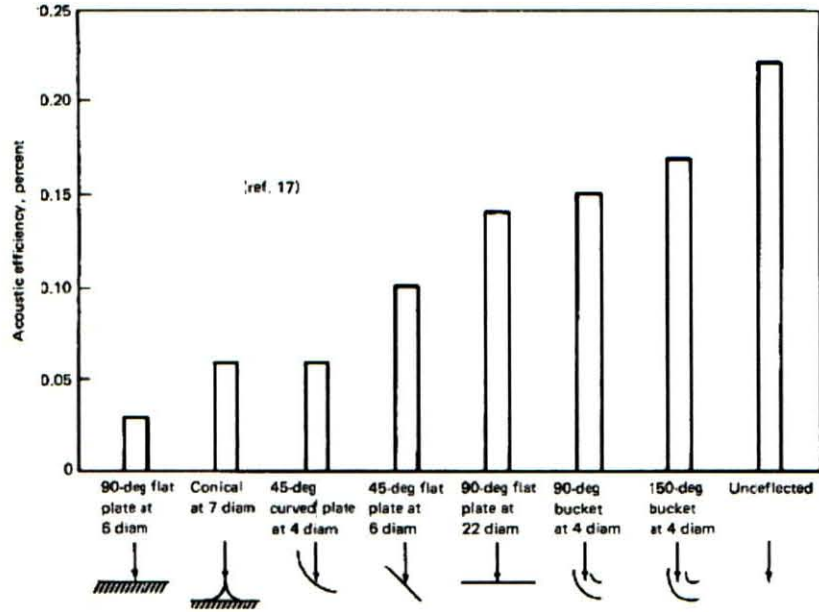


Figure 8: Acoustic efficiency of various plume deflections [2]

The overall sound power is then found using the efficiency factored against the mechanical power [4],

$$W_{OA} = \eta F V_e \quad \text{Eq. 9}$$

The overall sound power can then be translated into an overall sound pressure level [2],

$$L_w = 10 \log(W_{OA}) + 120 \quad \text{Eq. 10}$$

Once the plume metrics are known, the plume is discretized into several slices and Strouhal numbers are found for each plume slice using the flow variables and choosing a frequency range (typically  $10^0$ - $10^4$  Hz),

$$S_n(s) = \frac{f s a_e}{V_e a_{amb}} \quad \text{Eq. 11}$$

The normalize overall sound power of each slice is found,

$$10 \log \left( x_t \frac{W(s)}{W_{OA}} \right) = 10 \log \left[ \frac{c_1 \left( \frac{s}{x_t} \right)^{c_2}}{\left( 1 + c_3 \left( \frac{s}{x_t} \right)^{c_4} \right)^{c_5}} \right] \quad \text{Eq. 12}$$

where  $c_1$ ,  $c_2$ ,  $c_3$ ,  $c_4$ , and  $c_5$  are correlation coefficients (omitted for SBU considerations). The strongest source typically sits between 1.5-2 core lengths from the exit plane (shown in figure below). The core (inviscid) region terminates ( $x_t$ ) when the jet-edge shear layers collapse and form a large turbulent zone in the plume. This is also the cause of the log reduction in axial velocity along the plume axis.

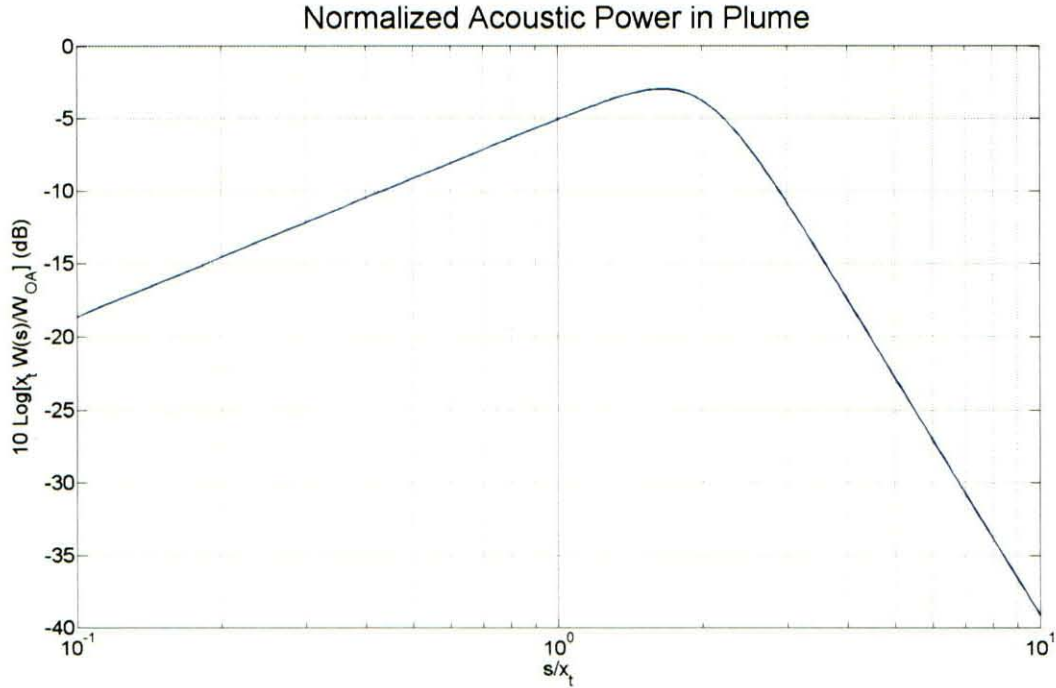


**Figure 9:** Normalized overall sound power along plume

The overall acoustic power for each slice is found [2],

$$L_{w,ps} = 10 \log \left[ \frac{x_t W(s)}{W_{OA}} \right] + L_w + 10 \log \left( \frac{\Delta x_t(s)}{x_t} \right) \quad \text{Eq. 13}$$

Knowing the Strouhal number range, the normalized power spectrum is found for each plume slice,

$$10 \log \left( W(f,s)/W(s) \left[ \frac{V_e a_{amb}}{s a_e} \right] \right) = 10 \log \left( \frac{c_1 S_n(s)^{c_2}}{1 + c_3 S_n(s)^{c_4}} \right) \quad \text{Eq. 14}$$

where  $c_1$ ,  $c_2$ ,  $c_3$ , and  $c_4$  are correlation coefficients (omitted for SBU considerations). An important caveat to these empirical correlations is that their coefficients are dependent on the propulsion type (chemical, nuclear, etc).

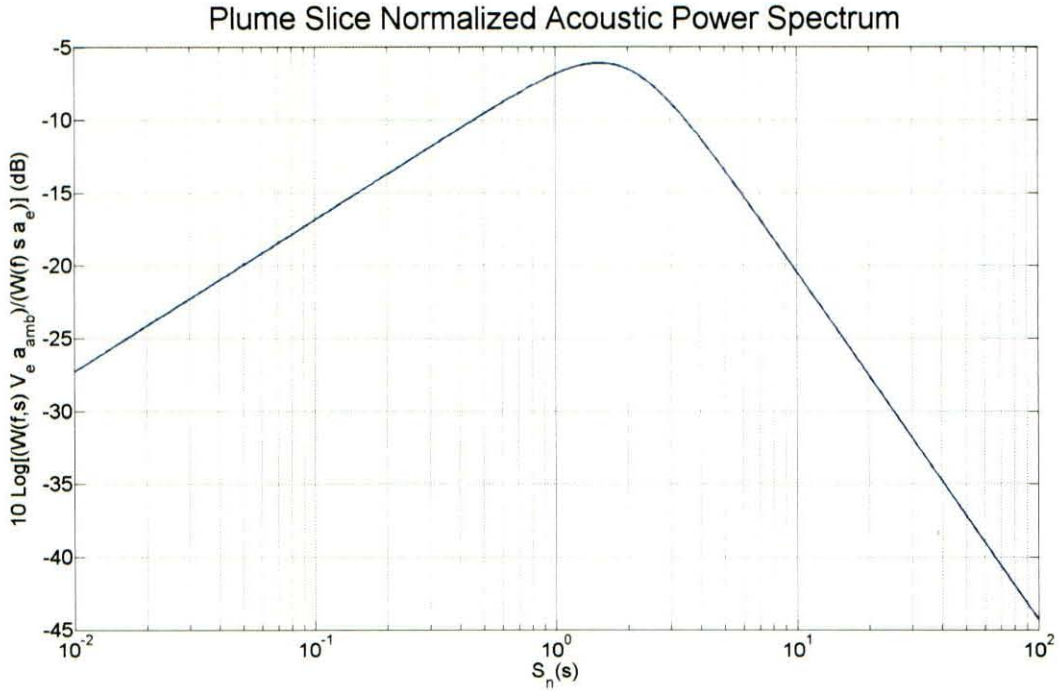


**Figure 10:** Normalized power spectrum of plume slice

The power spectrum for each plume slice is then found [2],

$$L_{w,ps,f} = 10 \log \left( W(f,s) / W(s) \left[ \frac{V_e a_{amb}}{s a_e} \right] \right) + L_{w,ps} - 10 \log \left( \frac{V_e a_{amb}}{s a_{amb}} \right) + 10 \log (\Delta f) \quad \text{Eq. 15}$$

The directivity indices are found by determining the true angles the receiver location makes with each plume slice.

The true angles are then converted to equivalent angles correcting for Strouhal number effects,

$$\beta_{eff} = \beta - c_1 \log (c_2 S_n(s)) \quad \text{Eq. 16}$$

where  $c_1$  and  $c_2$  are correlation coefficients (omitted for SBU considerations). Knowing the effective angle, directivity index is computed,

$$DI(\beta_{eff}) = 10 \log \left[ \frac{c_1 + c_2 \cos^4(\beta_{eff})}{[(1 - c_3 \cos(\beta_{eff}))^{c_4} + c_5]^{c_6} [1 + c_7 \exp(c_8 \beta_{eff})]} \right] - c_9 \log(S_n(s)) - c_{10} \quad \text{Eq. 17}$$

where  $c_1, c_2, c_3, c_4, c_5, c_6, c_7, c_8, c_9,$  and  $c_{10}$  are correlation coefficients (omitted for SBU considerations). The average (over a typical Strouhal number range) directivity of chemical rockets it's approximately  $40^\circ$  (see figure below).

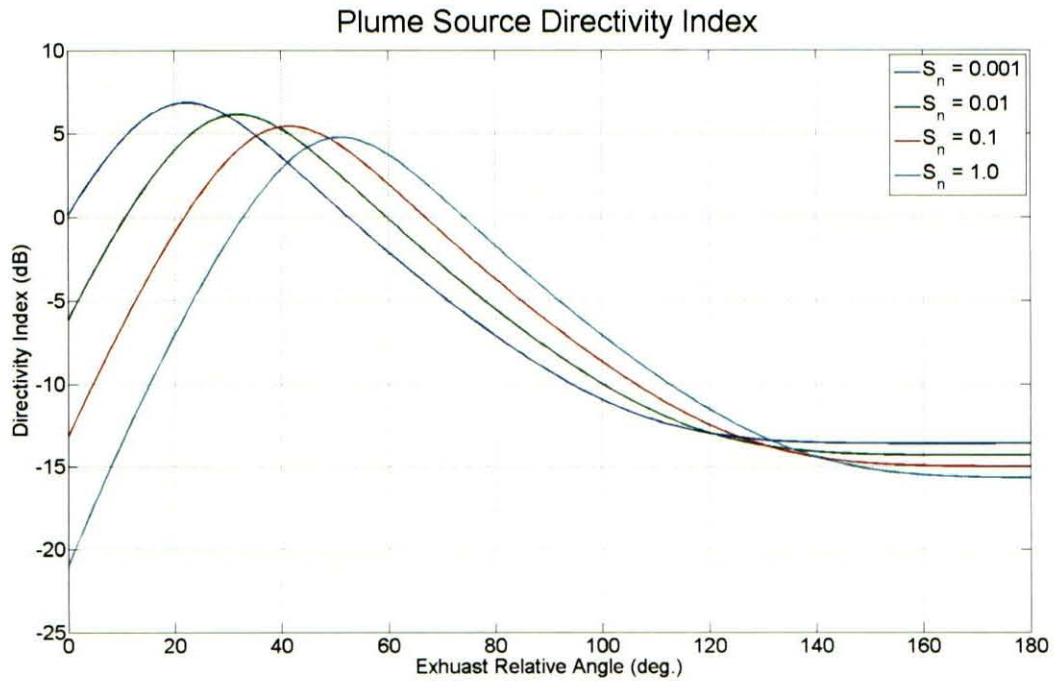


**Figure 11:** Acoustic source directivity index (at various Strouhal numbers)

Again, the coefficients vary for different propulsion types. The mean directivity for various propulsion sources is shown in the figure below.

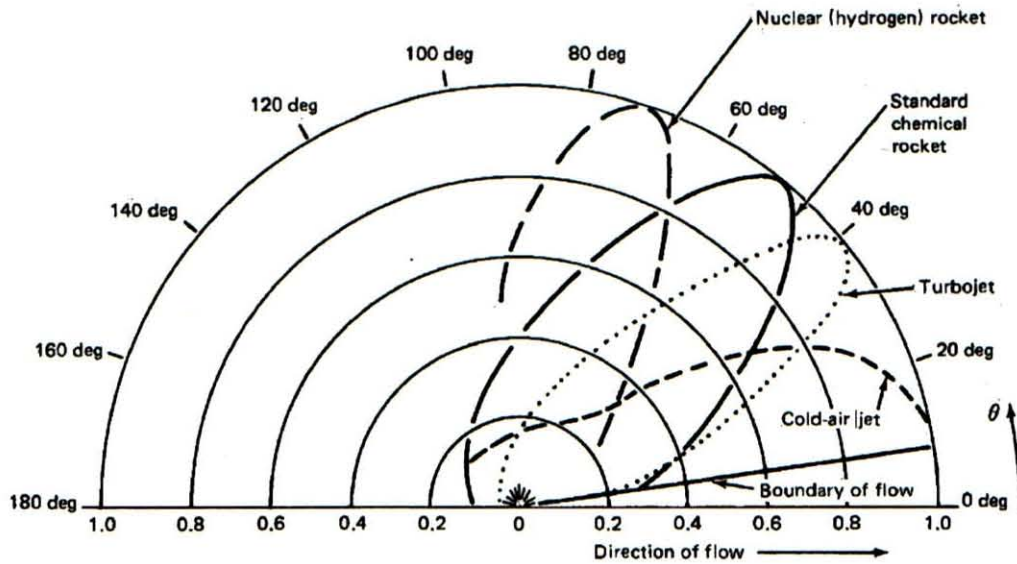


**Figure 12:** Directional characteristics for various propulsion types [2]

The frequency dependant sound pressure level from each plume slice for a receiver is [2],

$$SPL_{ps,f} = L_{w,ps,f} - 10 \log(R^2) - 11 + DI(\beta_{eff}) \quad \text{Eq. 18}$$

A logarithmic summation over all plume slices of the above will yield the sound pressure spectrum for a receiver [2],

$$SPL_f = 10 \log \left( \sum 10^{\frac{SPL_{ps,f}}{10}} \right) \quad \text{Eq. 19}$$

The overall sound pressure level for a receiver can be found from another logarithmic summation over the entire spectrum [2],

$$OASPL = 10 \log \left( \sum 10^{\frac{SPL_f}{10}} \right) \quad \text{Eq. 20}$$

Corrections to the sound pressure spectrum for ear sensitivity can be done by including the A-weighted term with the  $SPL_{ps,f}$  equation,

$$SPL_{f,A_w} = SPL_f + A_w(f) \quad \text{Eq. 21}$$

The A-weighted correction for the human ear is frequency dependant [4],

$$R_A(f) = \frac{12200^2 f^4}{(f^2 + 20.6^2) \sqrt{(f^2 + 107.7^2)(f^2 + 737.9^2)} (f^2 + 12200^2)} \quad \text{Eq. 22}$$

$$A_w(f) = 2.0 + 20 \log(R_A(f)) \quad \text{Eq. 23}$$

Summation of  $SPL_{f,A_w}$  will give the OASPL in dBA.

Corrections to the sound pressure spectrum (normal not A-weighted) for diffraction with a wall can be done by including the diffraction term with the  $SPL_{ps,f}$  equation. An empirical correlation used to determine the diffracted gain in the acoustic spectrum (see figure below).

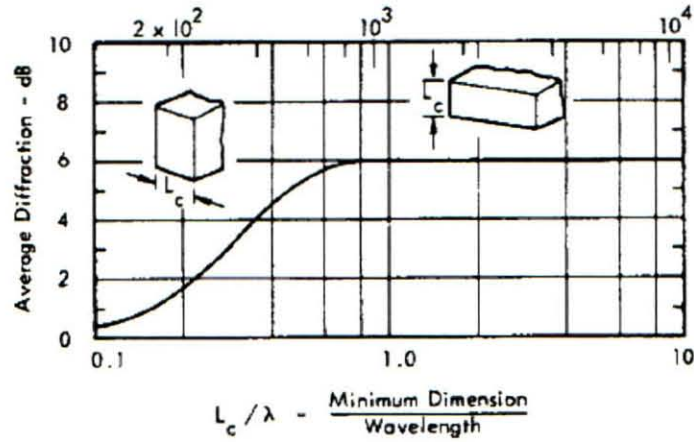


**Figure 13:** Diffracted gain versus non-dimensional characteristic length [5]

The non-dimensional characteristic length can be converted to frequency by,

$$f = \left( \frac{L_c}{\lambda} \right) \frac{a}{L_c} \quad \text{Eq. 24}$$

The acoustic spectrums are then corrected for diffraction by applying the correlation,

$$SPL_{f,diff} = SPL_f + DIFF(f) \quad \text{Eq. 25}$$

The diffracted acoustic spectrums are then applied to all walls of the facility.

$$SPL_{f,inner} = SPL_{f,diff} - 10 \log_{10} \left( \frac{1}{\bar{\tau}} \right) + 10 \log_{10} \left( \frac{A(1 - \bar{\alpha})}{S\bar{\alpha}} \right) \quad \text{Eq. 26}$$

In the above equation, the second term is the transmission loss (TL; from wall and windows) and third is the absorption loss (from internal carpeting, cubicles, etc).

The average transmissivity is found by taking an area-weighted average for all walls. The transmission loss is depended on the wall fundamental and critical frequency,

$$f_0 = \frac{\pi}{2} \sqrt{\frac{Et^3}{12m(1 - \nu^2)}} \left[ \left( \frac{1}{L^2} \right) + \left( \frac{1}{W^2} \right) \right] \quad \text{Eq. 27}$$

$$f_c = \frac{c^2}{2\pi} \sqrt{\frac{m(12(1 - \nu^2))}{Et^3}} \quad \text{Eq. 28}$$

The transmission loss is also largely dependent on the wall type (single or double panel wall). For a single panel wall,

$$\begin{aligned}
 \frac{f}{f_c} \leq \frac{f_0}{f_c} &\longrightarrow TL = 0 \text{ dB} \\
 \frac{f_0}{f_c} < \frac{f}{f_c} \leq \frac{1.5f_0}{f_c} &\longrightarrow TL = \left( \frac{20 \log_{10} \left( \frac{\pi \eta f_c}{\rho x l} \right) + 20 \log_{10} \left( \frac{1.5 f_0}{f_c} \right) - 5.5}{\log_{10} \left( \frac{1.5 f_0}{f_c} \right) - \log_{10} \left( \frac{f_0}{f_c} \right)} \right) \left( \log_{10} \left( \frac{f}{f_c} \right) - \log_{10} \left( \frac{f_0}{f_c} \right) \right) \text{ dB} \\
 \frac{1.5f_0}{f_c} < \frac{f}{f_c} \leq 0.5 &\longrightarrow TL = 20 \log_{10} \left( \frac{\pi f_c m}{\rho x l} \right) + 20 \log_{10} \left( \frac{f}{f_c} \right) - 5.5 \text{ dB} \\
 0.5 < \frac{f}{f_c} \leq 1.0 &\longrightarrow TL = \left( \frac{10 \log_{10} \left( \frac{2\eta}{\pi} \right) - 20 \log_{10} (0.5) + 5.5}{-\log_{10} (0.5)} \right) \left( \log_{10} \left( \frac{f}{f_c} \right) - \log_{10} (0.5) \right) + 20 \log_{10} \left( \frac{\pi \eta f_c}{\rho x l} \right) + 20 \log_{10} (0.5) - 5.5 \text{ dB} \\
 1.0 < \frac{f}{f_c} \leq \frac{f_d}{f_c} &\longrightarrow TL = 20 \log_{10} \left( \frac{\pi f_c m}{\rho x l} \right) + 20 \log_{10} \left( \frac{f}{f_c} \right) + 10 \log_{10} \left( \frac{2\eta f}{\pi f_c} \right) \text{ dB} \quad f_d = \left( \frac{\pi f_c}{2\eta} \right) [10^{-0.55}] \\
 \frac{f_d}{f_c} < \frac{f}{f_c} &\longrightarrow TL = 20 \log_{10} \left( \frac{\pi f_c m}{\rho x l} \right) + 20 \log_{10} \left( \frac{f}{f_c} \right) - 5.5 \text{ dB}
 \end{aligned}$$

Eq. 29

It is important to note that the method conservatively assumes there is no transmission loss below the fundamental frequency of the panel. This was done primarily because specific treatment of this region was not taken into account being that the sound field is diffuse [11].

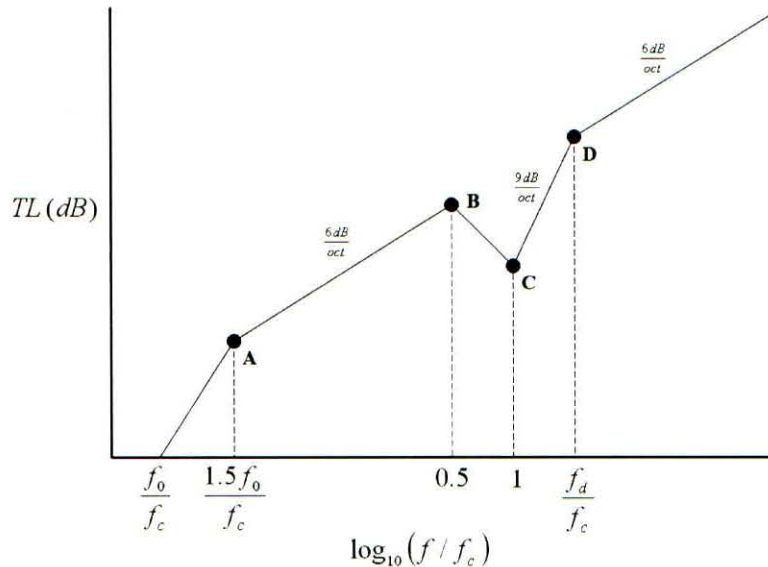


**Figure 14:** Typical transmission loss profile for a single panel wall

For double wall constructions, the analysis methodology is significantly different. First, the calculations for the method must be done in metric units. This is due to several simplifications that were included in the development of



the procedure by Bies and Hansen [11]. Secondly, since double wall constructions can contain an air space, the equation for the fundamental frequency changes to account for coupling effects [8],

$$f_0 = 80 \sqrt{\frac{(m_1 + m_2)}{d(m_1 m_2)}} \quad \text{Eq. 30}$$

Once this frequency is determined, it then becomes necessary to determine the critical frequency of both wall panels [8],

$$f_{c_{1,2}} = \frac{c^2}{2\pi} \sqrt{\frac{m_{1,2} (12 (1 - (v_{1,2})^2))}{E_{1,2} (t_{1,2})^3}} \quad \text{Eq. 31}$$

where if any wall panel is made of thin, equal-thickness sheets of material sandwiching a lightweight core, the critical frequency equation changes to [8],

$$f_{c_{1,2}} = \frac{c^2}{2\pi} \sqrt{\frac{m_{1,2} (2 (1 - (v_{1,2})^2))}{E_{1,2} t_{1,2} (t_{p_{1,2}} - t_{1,2})^2}} \quad \text{Eq. 32}$$

It is important to note that the subscripts 1 and 2 in these equations correspond to the panel with the lowest critical frequency and highest critical frequency, respectively. The general transmission loss spectrum for a double panel construction is shown in the figure below.

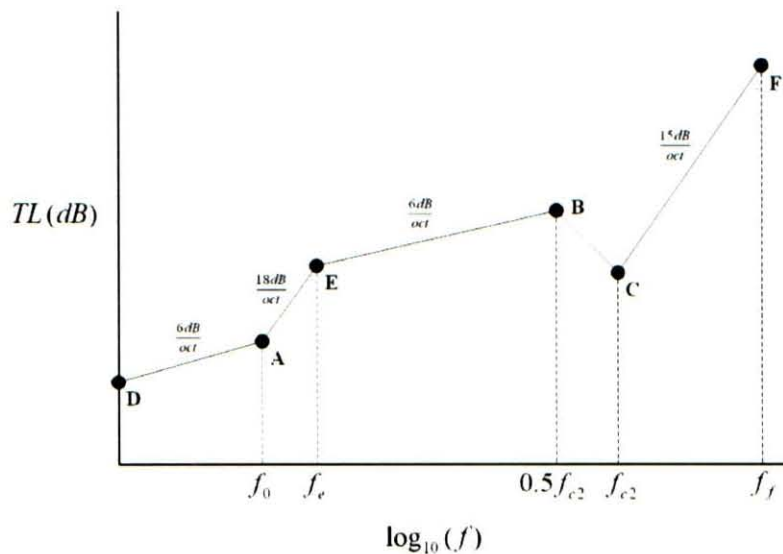


**Figure 15:** Typical transmission loss profile for double panel wall

For a double panel wall the transmission loss is found from,

$$\begin{aligned}
0 &\longrightarrow D = 10 \log_{10} \left[ \left( f^{\left( \frac{6}{\log_{10}(2)} \right)} \right) \left( 10^{\left( \frac{-6}{\log_{10}(2)} \log_{10}(f_0) + 20 \log_{10}(m_1 + m_2) + 20 \log_{10}(f_0) - 48 \right)} \right) \right] dB \\
0 \leq f_0 &\longrightarrow \text{LINEAR INTERPOLATION USED} \\
f_0 &\longrightarrow A = 20 \log_{10}(m_1 + m_2) + 20 \log_{10}(f_0) - 48 \text{ dB} \\
f_0 < f \leq f_e &\longrightarrow \text{LINEAR INTERPOLATION USED} \\
f_e &\longrightarrow E = 60(\log_{10}(f_e) - \log_{10}(f_0)) + 20 \log_{10}(m_1 + m_2) + 20 \log_{10}(f_0) - 48 \text{ dB} \quad f_e = 10^{\left( \frac{B - A + 60 \log_{10}(f_0) - 20 \log_{10}(0.5f_{c2})}{40} \right)} \\
f_e < f \leq 0.5f_{c2} &\longrightarrow \text{LINEAR INTERPOLATION USED} \\
0.5f_{c2} &\longrightarrow \begin{aligned} B_1 &= 20 \log_{10}(m_1 + m_2) + 20 \log_{10}(f_0) - 48 + 20 \log_{10} \left( \frac{f_{c1}}{f_0} \right) - 6 \text{ dB} \\ B_2 &= 20 \log_{10}(m_1) + 10 \log_{10}(b) - 48 + 30 \log_{10}(f_{c2}) + 20 \log_{10} \left[ 1 + \frac{m_2 \sqrt{f_{c1}}}{m_1 \sqrt{f_{c2}}} \right] - 78 \text{ dB} \end{aligned} \\
0.5f_{c2} < f \leq f_{c2} &\longrightarrow \text{LINEAR INTERPOLATION USED} \\
f_{c2} &\longrightarrow \begin{aligned} C_1 &= B + 6 + 1 - \log_{10}(\eta_2) \text{ dB} && (\text{if } f_{c2} \neq f_{c1}) \\ C_2 &= B + 6 + 1 - \log_{10}(\eta_2) + 5 \log_{10}(\eta_1) \text{ dB} && (\text{if } f_{c2} = f_{c1}) \end{aligned} \\
f_{c2} < f \leq f_f &\longrightarrow \text{LINEAR INTERPOLATION USED} \\
f_f &\longrightarrow F = \frac{15}{\log_{10}(2)} (\log_{10}(f_f) - \log_{10}(f_{c2})) + C \text{ dB} \quad f_f > f_{c2}
\end{aligned}$$

Eq. 33

An important aspect of the double wall calculation method is that linear interpolation is required to solve for the transmission loss at the frequency values between the known points. This is due to the fact that there are several possible combinations of equations that need to be used, depending on the boundary conditions of the wall/window being analyzed. An example of this is when calculating the transmission loss at point B on the spectrum. If the space between the two panels comprising the double wall construction contains no sound absorbing material, the value of  $B_1$  is used at point B; otherwise, the value at point B is the larger of  $B_1$  and  $B_2$ .

The average absorption coefficient is found by taking an area-weighted average of all individual absorption sources,

$$\bar{\alpha} = \frac{\alpha_i A_i + \alpha_{i+1} A_{i+1} + \dots + \alpha_n A_n}{A_i + A_{i+1} + \dots + A_n} \quad \text{Eq. 34}$$

Typical values for absorption coefficient are shown in the table below.

ACOUSTIC ABSORPTION COEFFICIENTS						
MATERIALS	125 HZ	250 HZ	500 HZ	1000 HZ	2000 HZ	4000 HZ
Painted Concrete:	0.1	0.05	0.06	0.07	0.09	0.08
Carpet:	0.01	0.05	0.10	0.20	0.45	0.65
Window Glass:	0.18	0.06	0.04	0.03	0.02	0.02
Linoleum Floor:	0.02	0.03	0.03	0.03	0.03	0.02
Ceiling Tiles:	0.30	0.51	0.80	0.85	0.78	0.66
Gypsum Board	0.29	0.10	0.06	0.05	0.04	0.04
Removable Walls	0.14	0.10	0.06	0.04	0.04	0.03

**Figure 16:** Typical values of absorption coefficient [10]

## VI. Sample Scenarios

Since CxP is the current NASA program, a sample case for the larger Ares-V heavy lift vehicle follows. In the scenario, an Ares-V vehicle is in the final stages (capping) of SRB stacking when an inadvertent ignition occurs. This event could happen in any of the four HB's. Because of this, the results are superimposed on all HB locations to determine the final SSD.

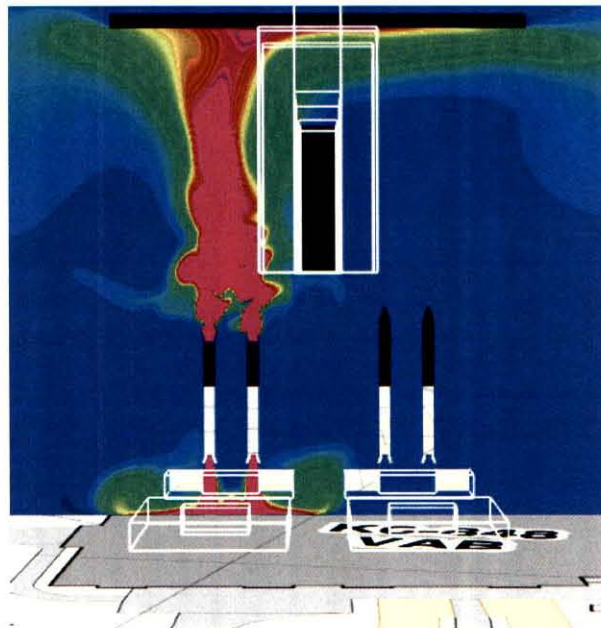


**Figure 17:** Sample case booster/plume configuration

The SRB segments are assumed to be identical to the SSP segments for this sample case. It's assumed that the chamber condition of these incomplete stacks is approximately 100 psia and 5000° F; the chamber gas specific heat ratio was assumed 1.17. Nozzle geometry used in the SSP SRB's was assumed along with the same SRB/ET sitting position on the ML in the VAB.

Because the boosters are uncapped, two plumes develop. The lower plume, because of the nozzle, has a larger exit Mach number ( $M_e \sim 2$ ) plume than the top plume ( $M_e = 1$ ). As a result, the lower plume sources are distributed farther out into the farfield and radiate sound further. In the near-field, the upper plume sound radiation is mainly confined to the VAB; little of its sound propagates to any significant area outside the VAB (see the figure below).

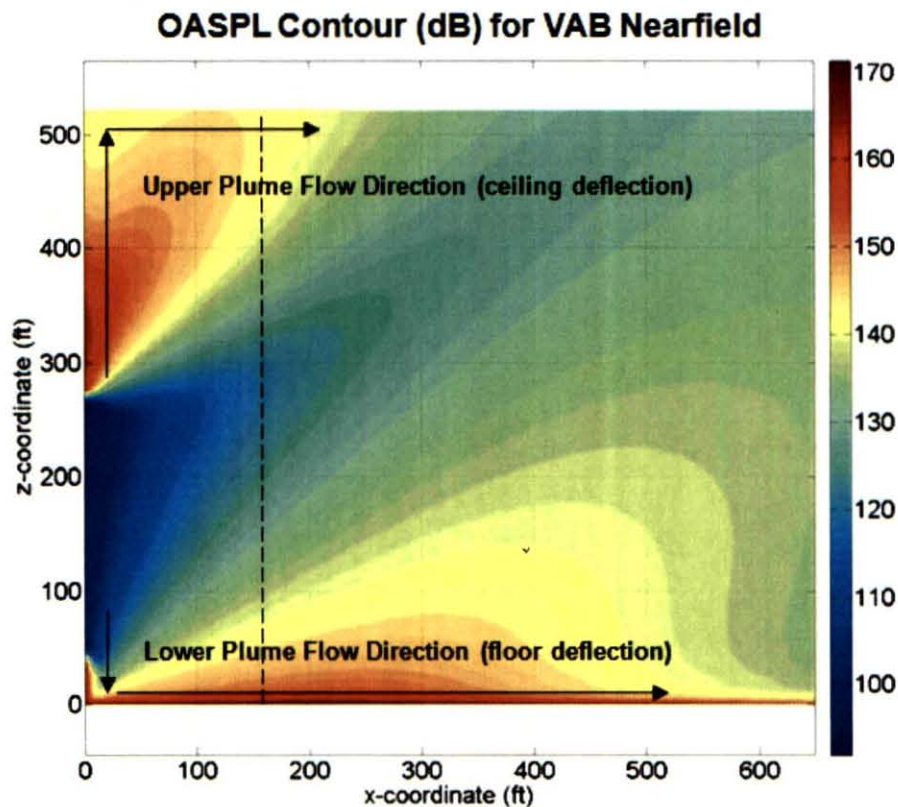


**Figure 18:** Near-field OASPL contour for sample case

In the farfield, the sound radiation is dominated mainly by the lower plume. After approximately 500 feet the OASPL decreases rapidly until it drops to insignificant levels past about 1000 feet (see the figure below).

### OASPL Contour (dB) for VAB Farfield (truncated to 0-100' elevation)

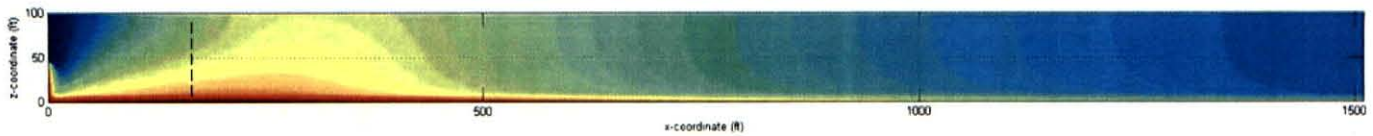


Figure 19: Farfield OASPL contour for sample case

The SSD is drawn below with the SSP QD arc discussed earlier. The SSD in the sample case sits well within the previous SSP QD arc (see the figure below).

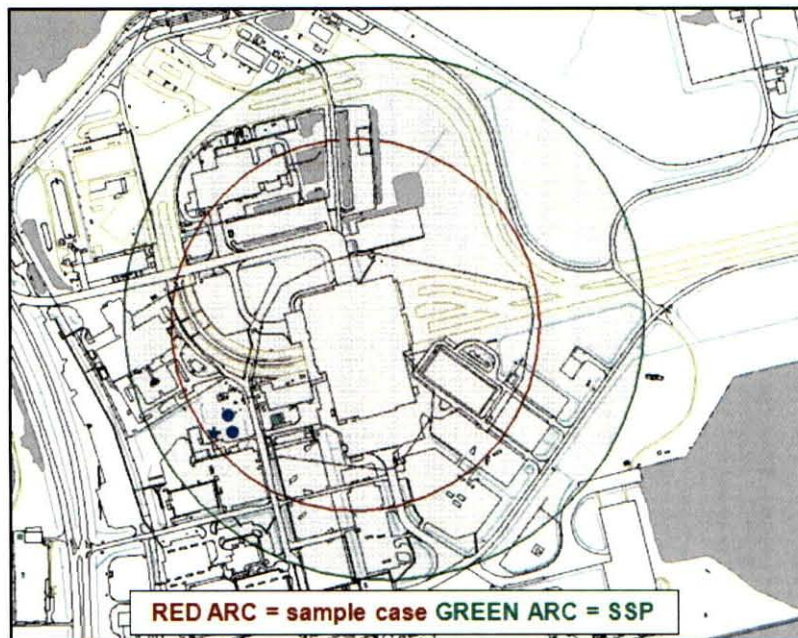


Figure 20: VAB area SSD plot for sample case ( $OASPL_{LCC} = 148$  dB,  $OASPL_{OPF-3} = 145$  dB)

From the transmission loss analysis, the LCC and OPF-3 impedances were not enough to reduce the OASPL below the 140 dB personnel limit; as a result these facilities would be unsafe as heavens.

## VII. Comments and Conclusions

A methodology for determining a SSD for aeroacoustic hazards has been successfully developed. Future improvements of the method could aim to reduce the conservatism (likely in the range of 10-20 dB). A new module is planned such to model the effectiveness of ear protection equipment. Furthermore, a module to parametrically model the effectiveness of facility barrier shielding is likely. The addition of these two new modules would add the dimension of mitigation to the model and methodology.

## Acknowledgments

The authors would like to thank Dr. Bruce Vu and Dr. Bob Youngquist for their help with the study.

## References

- 1 Heat Flux Based Assessment of Safe Separation Distances for Kennedy Space Center Vehicle Assembly Building (VAB) in Support of Constellation Mission Requirements, Vol. I. & Vol. II, August 2009 (internal).
- 2 Eldred, K.M.: Acoustic Loads Generated by the Propulsion System. NASA SP-8072, June 1971.
- 3 29 CFR 1910.95, Occupational Noise Exposure ([www.osha.gov](http://www.osha.gov))
- 4 Crocker, M.J.: Handbook of Acoustics. Auburn University, 1998.
- 5 Sutherland, L.C.: Sonic and Vibration Environments for Ground Facilities - A Design Manual. WR 68-2, March 1968.
- 6 Anderson, J.D.: Modern Compressible Flow. 3rd Edition, 2003.
- 7 Laney, R.C.: Environment Assessment of Vehicle Assembly Building During Accidental Ignition/Burning of Solid Rocket Motor Segments. TWR-11389-1, October 1978.
- 8 Sarafin, T. P.: Spacecraft Structures and Mechanisms: From Concept to Launch. 2003.
- 9 Hill, P.; Peterson, C.: Mechanics and Thermodynamics of Propulsion. 2nd Edition, 1992.
- 10 Barron, R. F.: Industrial Noise Control and Acoustics. 2003.
- 11 Bies, D. A.; Hansen C.: Engineering Noise Control: Theory and Practice. 3rd Edition, 2003.

# KSC VAB Aeroacoustic Hazard Assessment

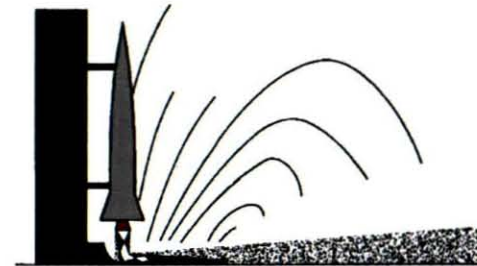
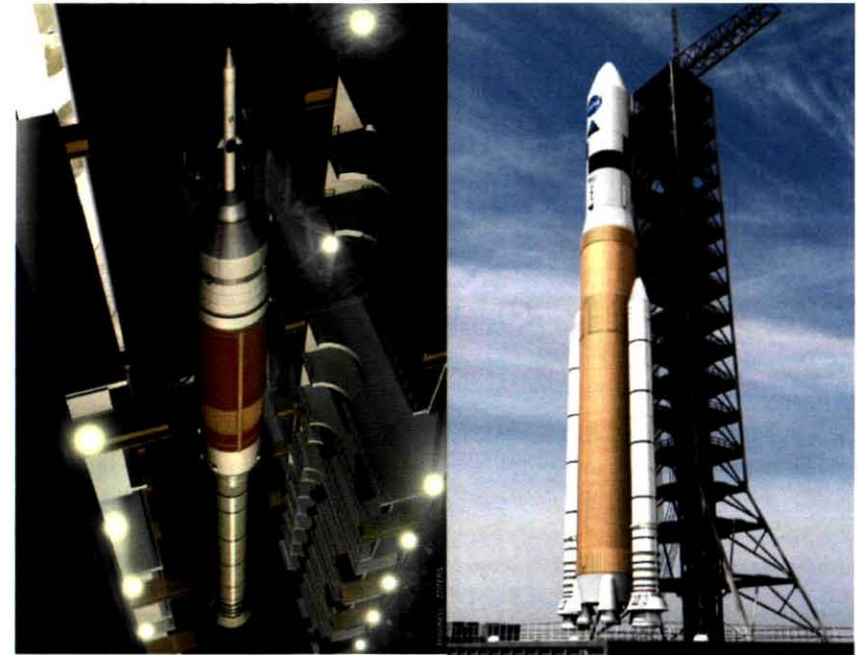
July 14, 2010

Justin M. Oliveira  
Analysis Branch, NE-M1  
NASA – KSC



# Outline

- Introduction**
- Assumptions**
- Model Overview**
- Calculation Methodology**
- Aeroacoustic Validation**
- Personnel Exposure Limit**
- Sample Scenario**
- Future Work**



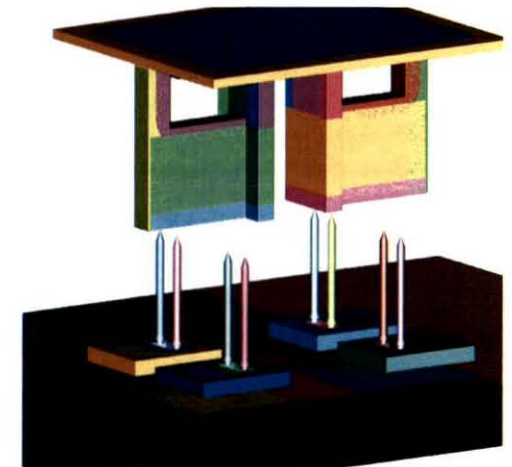
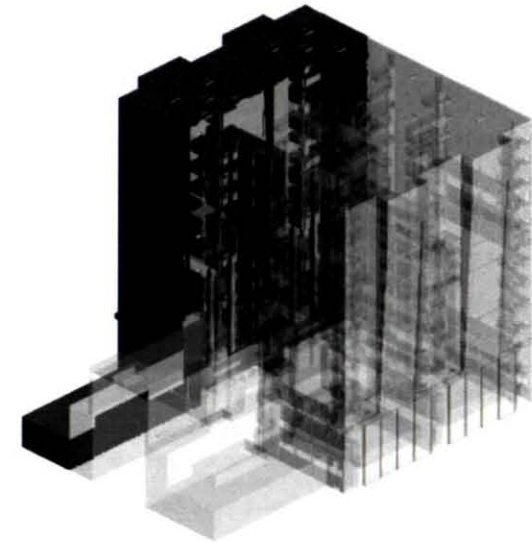


# Introduction

- In early 2007 efforts initiated to quantify inadvertent hazards in KSC processing areas for Constellation Program (CxP)
- Use of the weight-based approach methodology resulted in very large arcs
- Alternatively, hazards were laid out individually to be assessed
- Some of the hazards considered were blast/fragmentation, radiative heating, aeroacoustics, toxics
- End result was to determine a safe separation distance (SSD) for each individual hazard
- The inputs, assumptions, criterion, and results of each individual hazard analysis were reviewed by peer committee
- This presentation deals specifically with the Aeroacoustic hazard component

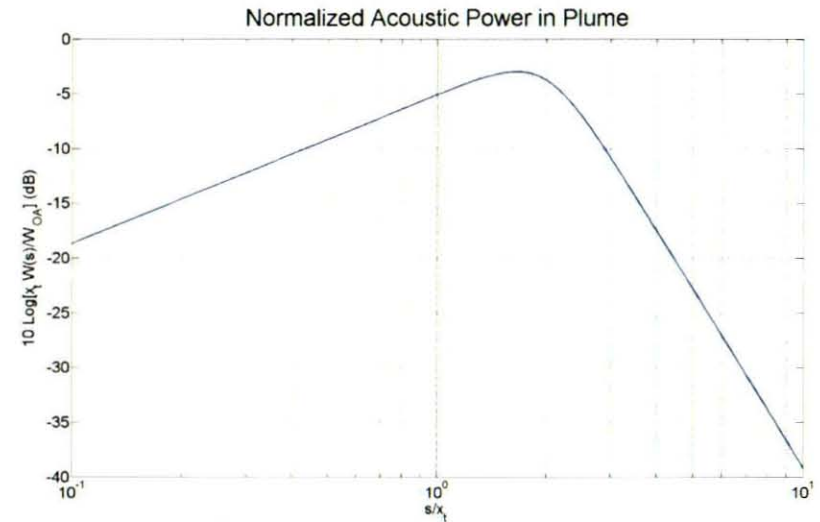
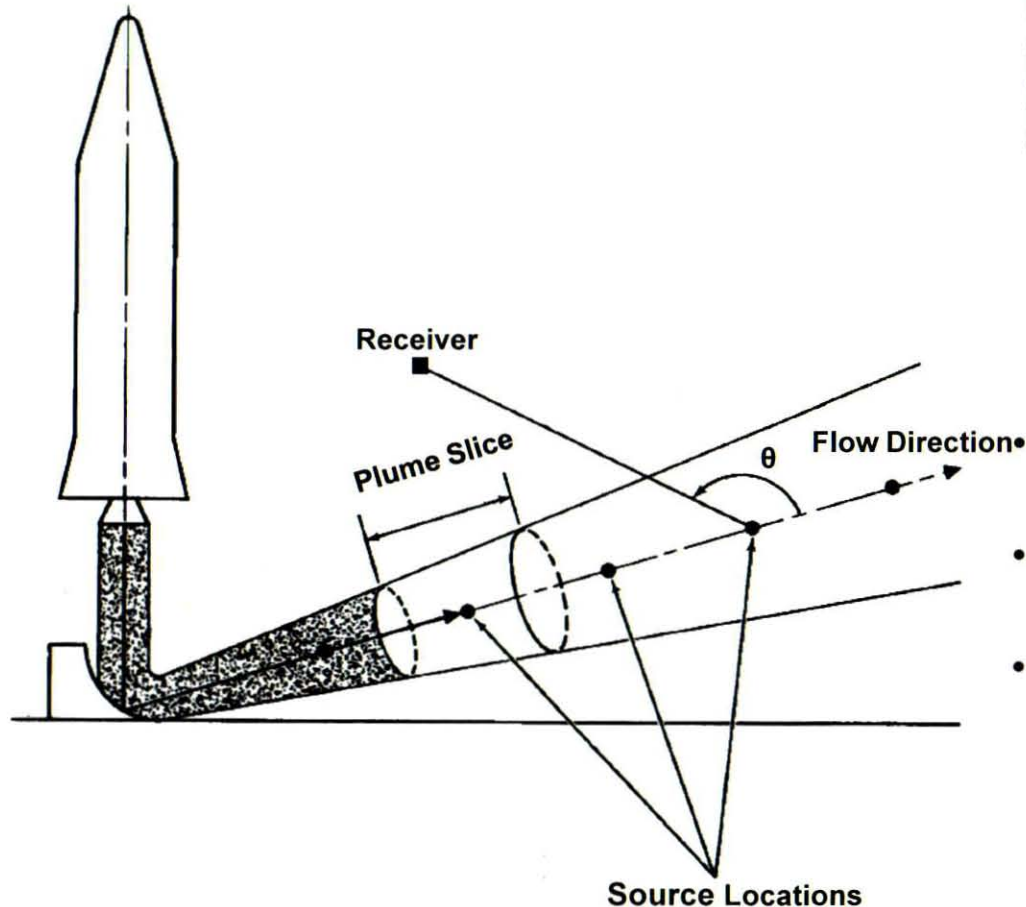
# Assumptions

- Burning stack/motor(s) are fixed in place and not pitched/tilted
- Assumed VAB paneling and internal-dividing walls removed
  - simplifies analysis
  - provides most conservative acoustic fields for farfield
- Plume(s) treated as axisymmetric
  - asymmetric spreading of the plume is not considered
- Adjacent plumes in close proximity conjoined
  - only if plumes within 1-5 exit diameters
  - sound powers combined to create one plume
- Neglected atmospheric sound absorption
  - effect negligible for small regions considered
  - provides small degree of conservatism to analysis
- Neglected ground reflections (other than initial plume deflection)
- Assumed incident acoustic load on facility normal and symmetric
- Facilities simplified to rectangles for diffraction analysis
- Walls and windows treated as simply supported panels
- At frequencies where absorption data unavailable, assumed no absorption
  - difficult to find building material data below 125 Hz
  - majority of rocket noise sits in the  $10^1 \sim 10^3$  Hz area
  - provides a large level of conservatism in analysis



# Model Overview

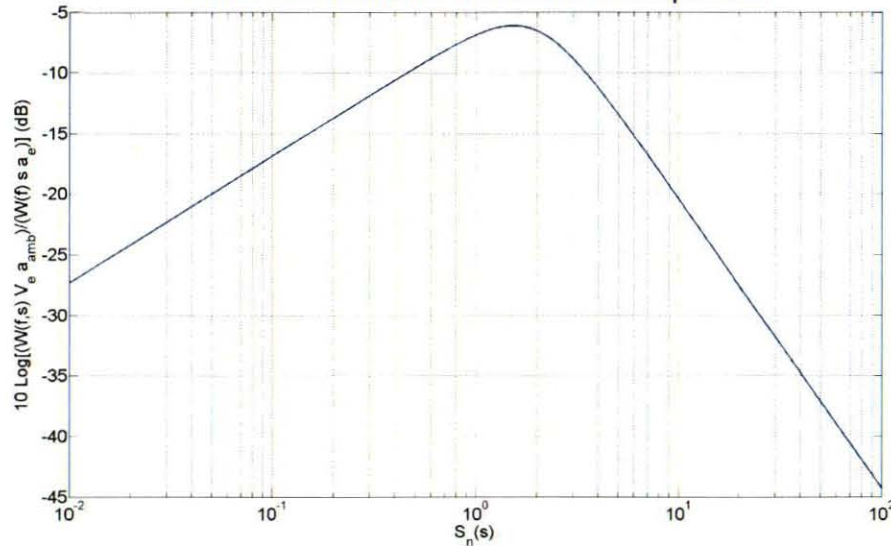
- Modified Eldred's Method
- Rocket plume divided into slices
- Each slice is treated a monopole source



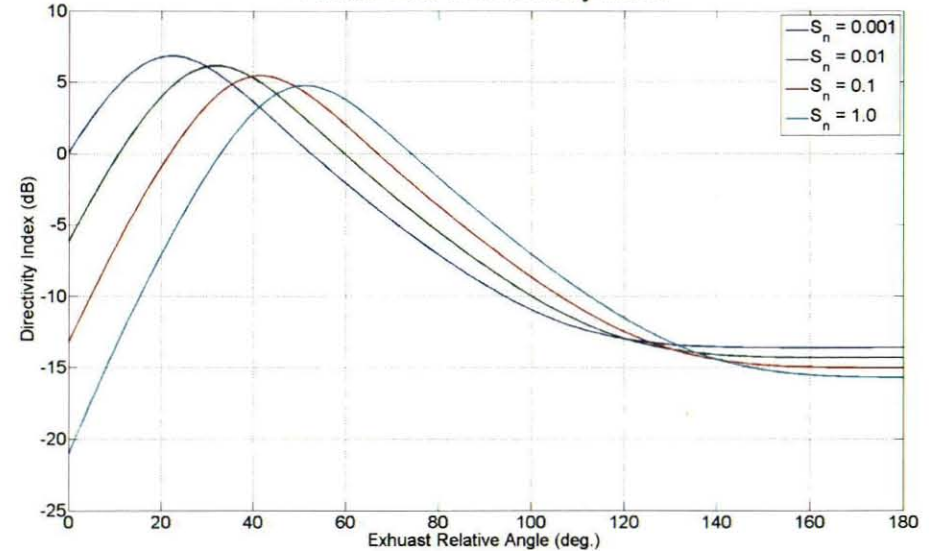
- Overall power of each slice dependant on location in plume
- Power maximum at  $\sim 1.5x$  core length (transitional region)
- Normalized converted to overall using,

$$L_{w,ps} = 10 \log \left[ \frac{x_t W(s)}{W_{OA}} \right] + L_w + 10 \log \left( \frac{\Delta x_t(s)}{x_t} \right)$$

Plume Slice Normalized Acoustic Power Spectrum



Plume Source Directivity Index



- Each source has spectrum dependant on plume strength (in form on Strouhal number)

- Normalized converted to overall using,

$$L_{w,ps,f} = 10 \log \left( W(f,s) / W(s) \left[ \frac{V_e a_{amb}}{s a_g} \right] \right) + L_{w,ps} - 10 \log \left( \frac{V_e a_{amb}}{s a_g} \right) + 10 \log (\Delta f)$$

- Directivity of source with receiver dependant on Strouhal number and true angle with plume flow direction; SPL at frequency for given receiver and source,

$$SPL_{ps,f} = L_{w,ps,f} - 10 \log(R^2) - 11 + DI(\beta_{sff})$$

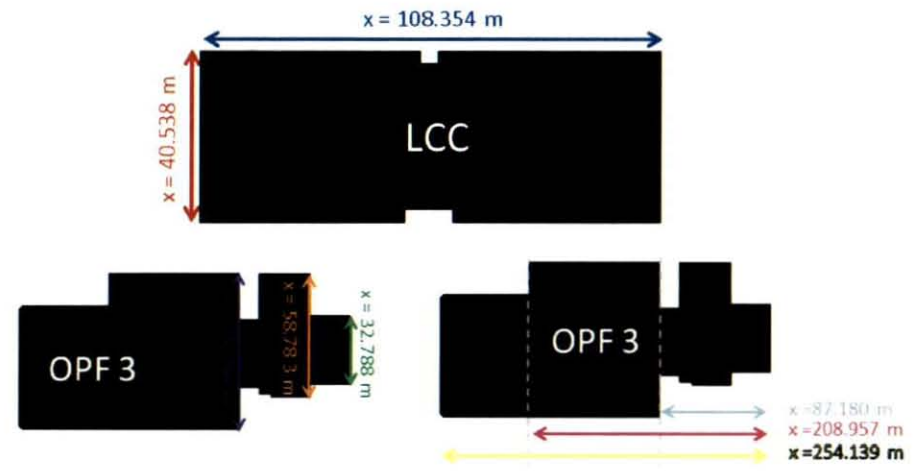
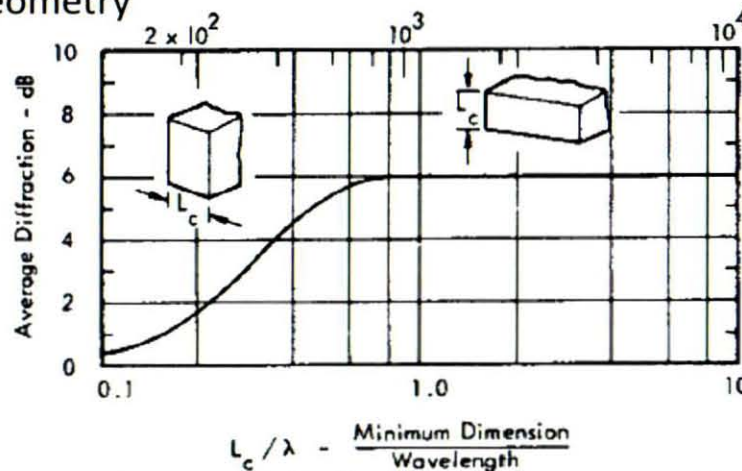
- For any given receiver, sound pressure from each source summed at each frequency; resulting in SPL spectrum for receiver,

$$SPL_f = 10 \log \left( \sum 10^{\frac{SPL_{ps,f}}{10}} \right)$$

- Receiver SPL spectrum integrated to find OASPL

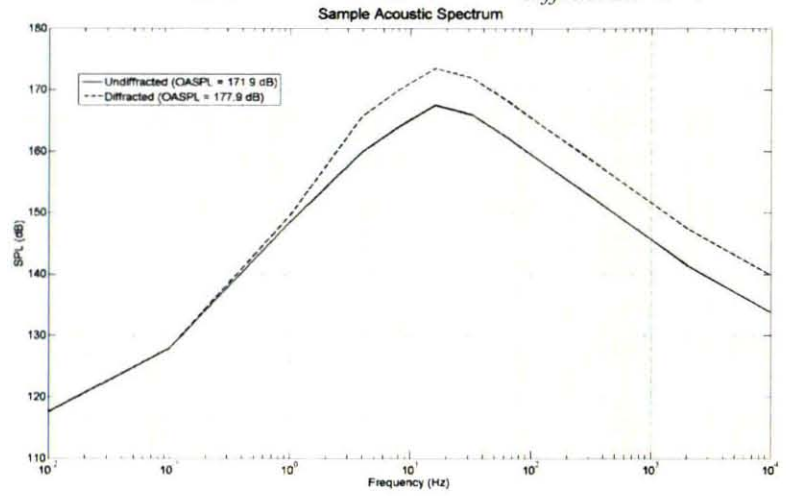
$$OASPL = 10 \log \left( \sum 10^{\frac{SPL_f}{10}} \right)$$

- The diffraction-gain spectrum is computed from semi-empirical correlations using the building geometry



- The spectrums at the facility distances are then corrected using the diffraction-gain spectrum to find the acoustic excitation on the facility wall for the transmission analysis

$$SPL^*(f) = SPL(f) + \Delta_{diffraction}(f)$$



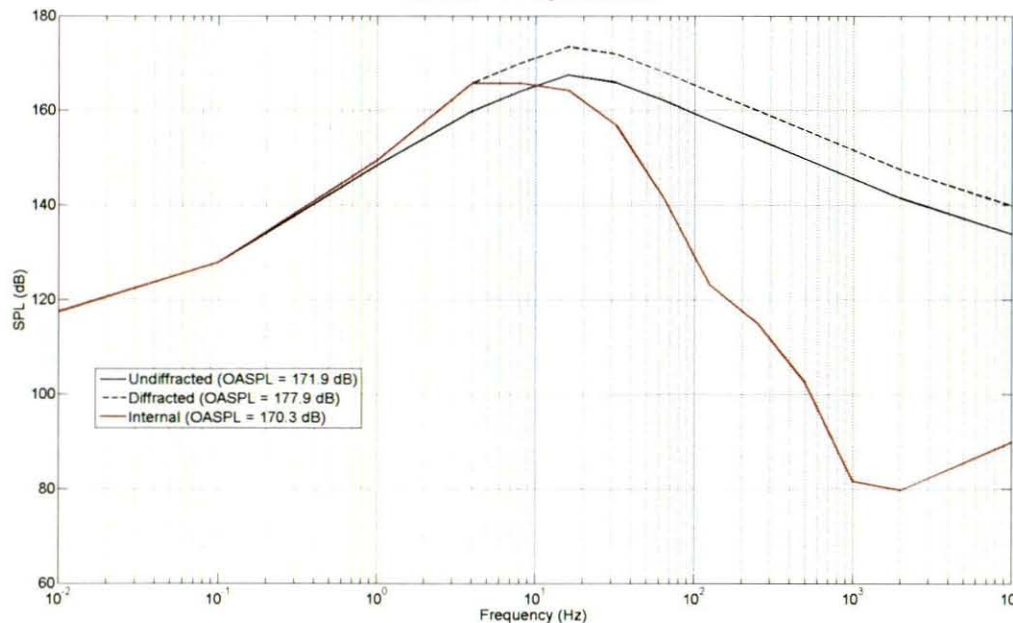
- Based on the facility geometry and composition, wall transmission and internal absorption losses are calculated

$$TL = 10 \log_{10} \left( \frac{1}{\bar{\tau}} \right) \quad AL = 10 \log_{10} \left( \frac{A(1 - \bar{\alpha})}{S\bar{\alpha}} \right)$$

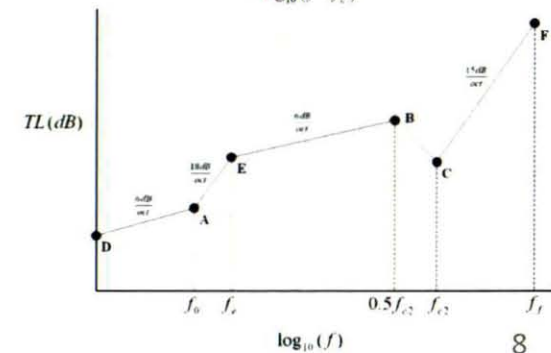
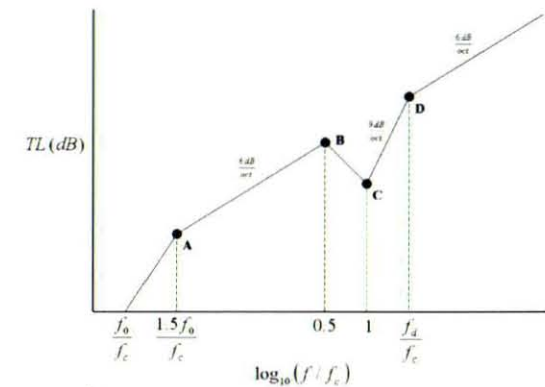
- Internal spectrum then computed by taking external diffracted spectrums and correcting for transmission/absorption losses

$$SPL' = SPL^* - TL + AL$$

Diffracted Spectrum



ACOUSTIC ABSORPTION COEFFICIENTS						
MATERIALS	125 HZ	250 HZ	500 HZ	1000 HZ	2000 HZ	4000 HZ
Painted Concrete:	0.1	0.05	0.06	0.07	0.09	0.08
Carpet:	0.01	0.05	0.10	0.20	0.45	0.65
Window Glass:	0.18	0.06	0.04	0.03	0.02	0.02
Linoleum Floor:	0.02	0.03	0.03	0.03	0.03	0.02
Ceiling Tiles:	0.30	0.51	0.80	0.85	0.78	0.66
Gypsum Board	0.29	0.10	0.06	0.05	0.04	0.04
Removable Walls	0.14	0.10	0.06	0.04	0.04	0.03



# Aeroacoustic Validation

- Modified Eldred's 2<sup>nd</sup> Method used for analysis
- Original method (NASA SP-8072) has been updated with new core and directivity correlations
- Super-position principle has been used to incorporate multiple non-conjoined plumes
- Method used to predict acoustics around launch pad under STS launches
- Method also used to predict launch acoustics for Ares-I/X
- Sample data shown to right for Ares-IX test flight on October 28, 2009 (data values not shown for ITAR/SBU considerations)
- Excellent agreement between model and measurements in the near and midfield spectrums;  $\pm 0.5$  dB
- Farfield spectrums from model over predict slightly in range of interest (10-1000 Hz);  $\pm 7$  dB
- OASPL values (not shown for ITAR/SBU considerations) between model and measurements for nearfield, midfield, and farfield off by only + 1 dB



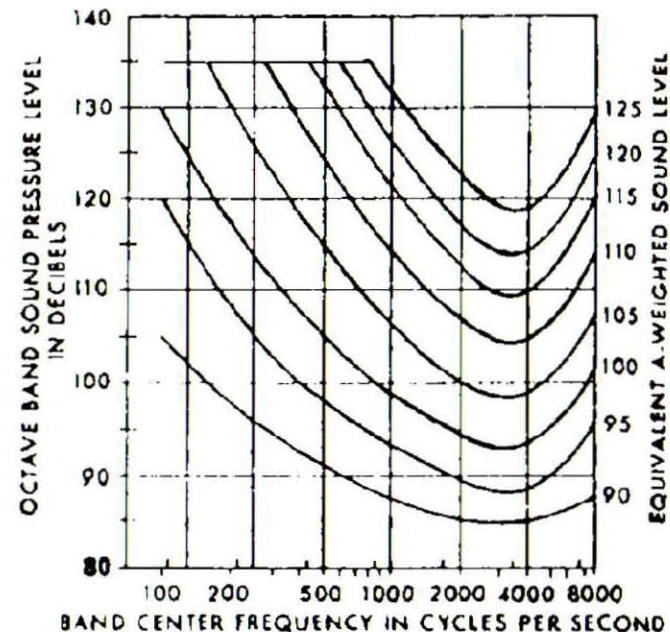
# Personnel Exposure Limit

- OSHA 1910.95(b)(2) would require a 115 dBA limit
  - OSHA table meant for industrial working environments and not inadvertent ignition events
  - Would result in overly conservative safe separation distances
- Practical limit would be that associated with onset of physical impediment
- Typical human ear threshold of pain occurs at 140 dB; ear drum rupture is typical at 160 dB
- Personnel exposure limit used was **140 dB** (OASPL); taken at conservative head level (5')

**OSHA 1910.95(b)(2)**

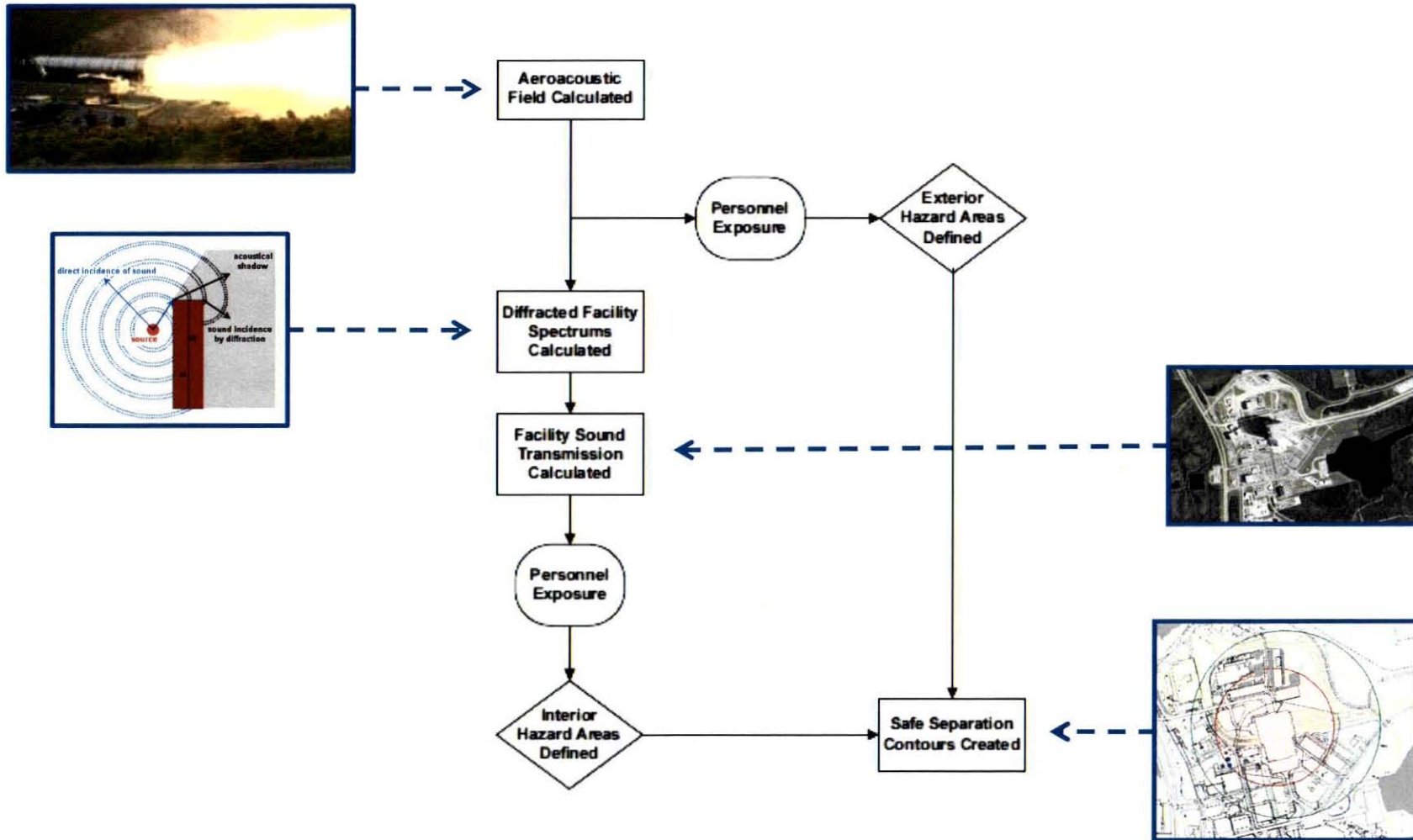
Duration Per Day, in Hours	Sound Level dBA, Slow Response
8	90
6	92
4	95
3	97
2	100
1-1/2	102
1	105
1/2	110
1/4 or less	115

**Note:** When the daily noise exposure is composed of two or more periods of noise exposure of different levels, their combined effect should be considered, rather than the individual effect of each.

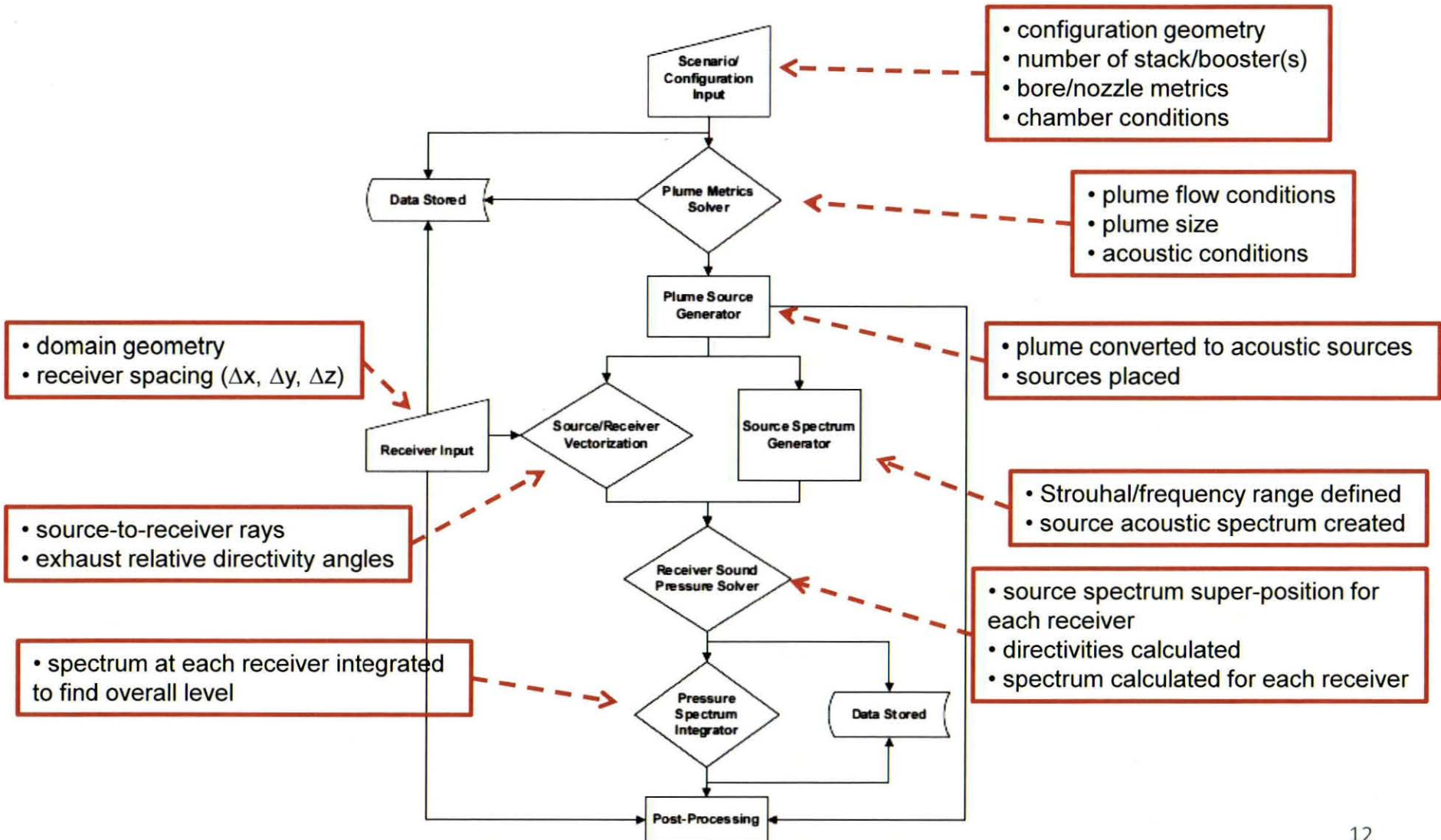




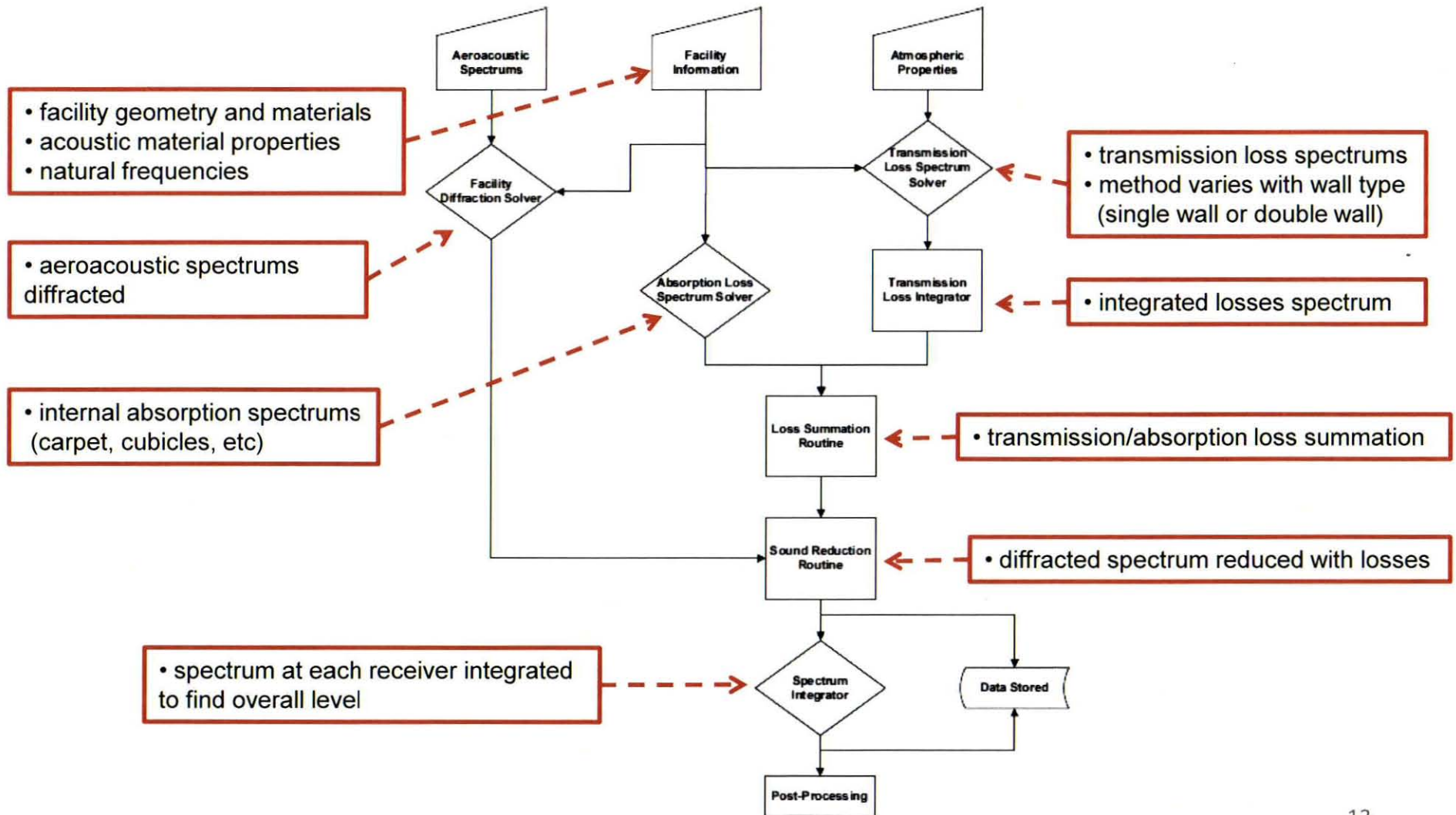
# Calculation Methodology



## Aeroacoustic Procedure

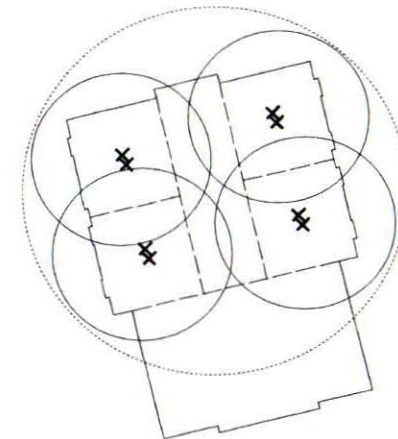
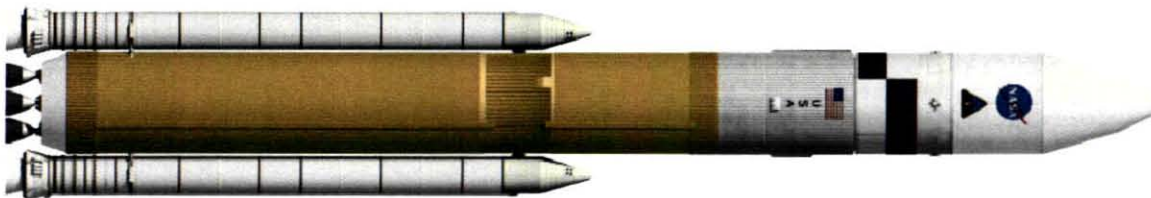
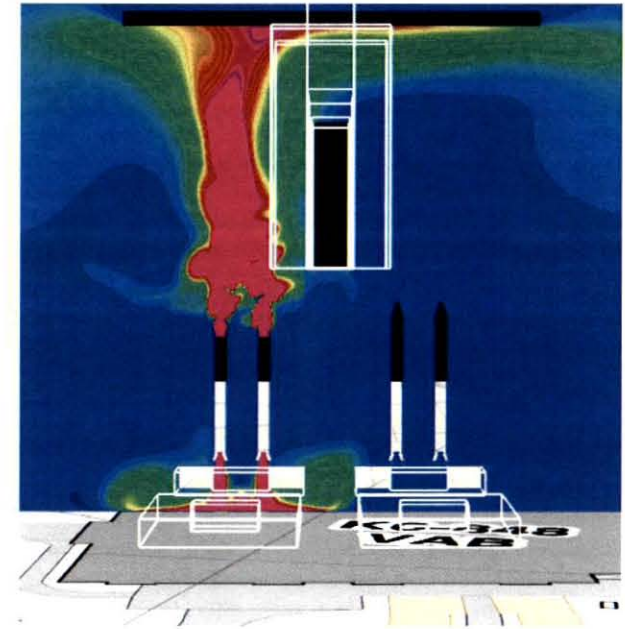


## Diffraction/Transmission Procedure

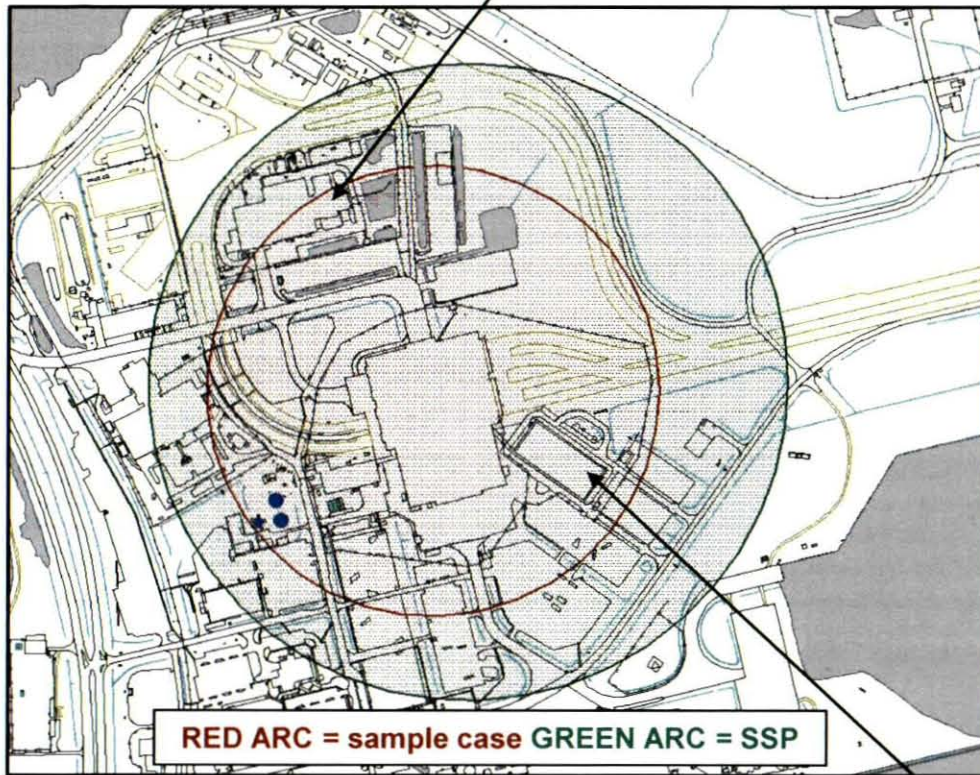


# Sample Scenario

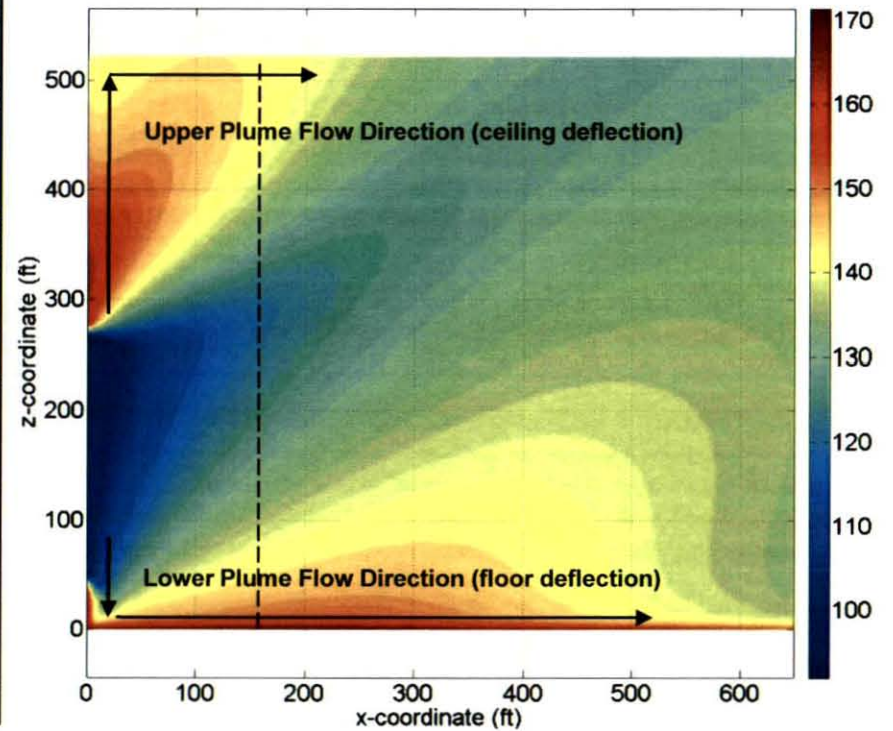
- VAB is 4<sup>th</sup> largest building in the world by volume
- Consists of 4 High Bays (HB) used to process vehicles (Shuttle, Ares-I, Ares-V)
- Ares-V vehicle uses (2) SRBs strapped to center stage
- SRBs are assembled first in VAB on ML piece-by-piece
- Sample scenario considers inadvertent ignition of (2) 4.5-segment stacks in a single HB
- Event could occur in any one of the HBs, so SSD calculated and placed at each HB center
- Final arc drawn from centroid of HBs such that all SSDs encompassed



OPF-3 OASPL = 145 dB (**UNSAFE**)

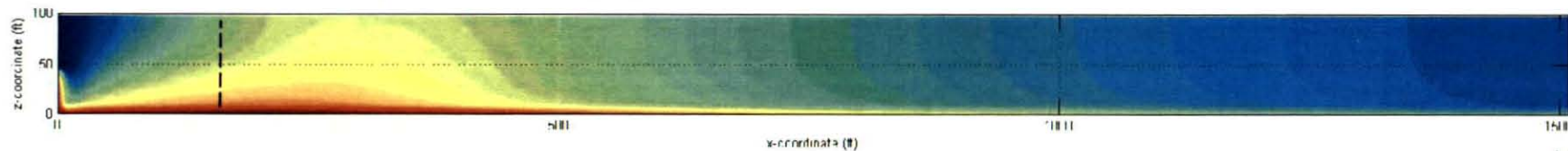


OASPL Contour (dB) for VAB Nearfield



LCC OASPL = 148 dB (**UNSAFE**)

OASPL Contour (dB) for VAB Farfield (truncated to 0-100' elevation)



# Future Work

- Obtain low frequency ( $< 125$  Hz) data for facility materials
  - either by experimental testing or computationally (FEA)
  - remove some conservatism from analysis
  - could be as much as 2-3 dB for certain facilities
- Develop ear plug/muff module using ANSI S12.68-2007 to better determine mitigation levels
  - better determine effectiveness of safety protection
  - better quantify effectiveness of certain equipment for rocket acoustic spectrums (10-1000 Hz)
- Parametric analysis of facility shielding
  - overlapping mitigation strategy from all hazard analyses involved blast shielding facilities in close proximity to VAB
  - analysis would determine effectiveness of shield size/construction to acoustic hazards
- Develop GUI for aeroacoustics code and register in NASA database
  - easier to obtain funding to support work if registered
  - could make available to other agencies or possibly open-source (ITAR restricted)

# Questions



# BACKUP SLIDES



## General Acoustics

## SOUND POWER LEVEL

$$L_w = 10 \log \left( \frac{W}{W_o} \right)$$

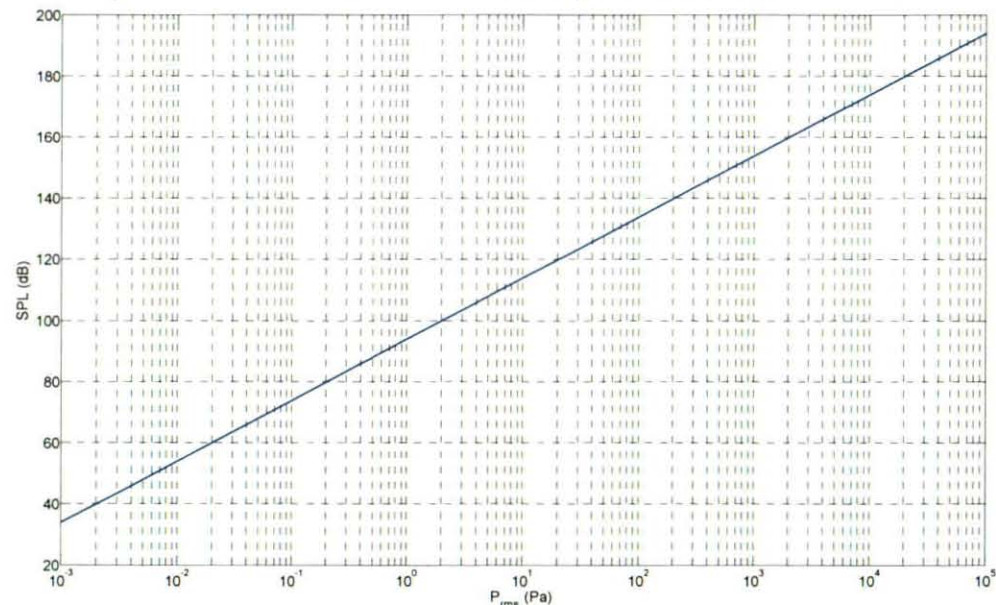
where  $W$  is the acoustic power (typically in aero-acoustics some percentage of the mechanical power),  
and  $W_o$  is the reference power (Watts)

## SOUND PRESSURE LEVEL

$$SPL = 20 \log \left( \frac{p}{p_o} \right)$$

where  $p$  is the root mean square (rms) pressure,  
and  $p_o$  is the reference rms pressure (Pa)

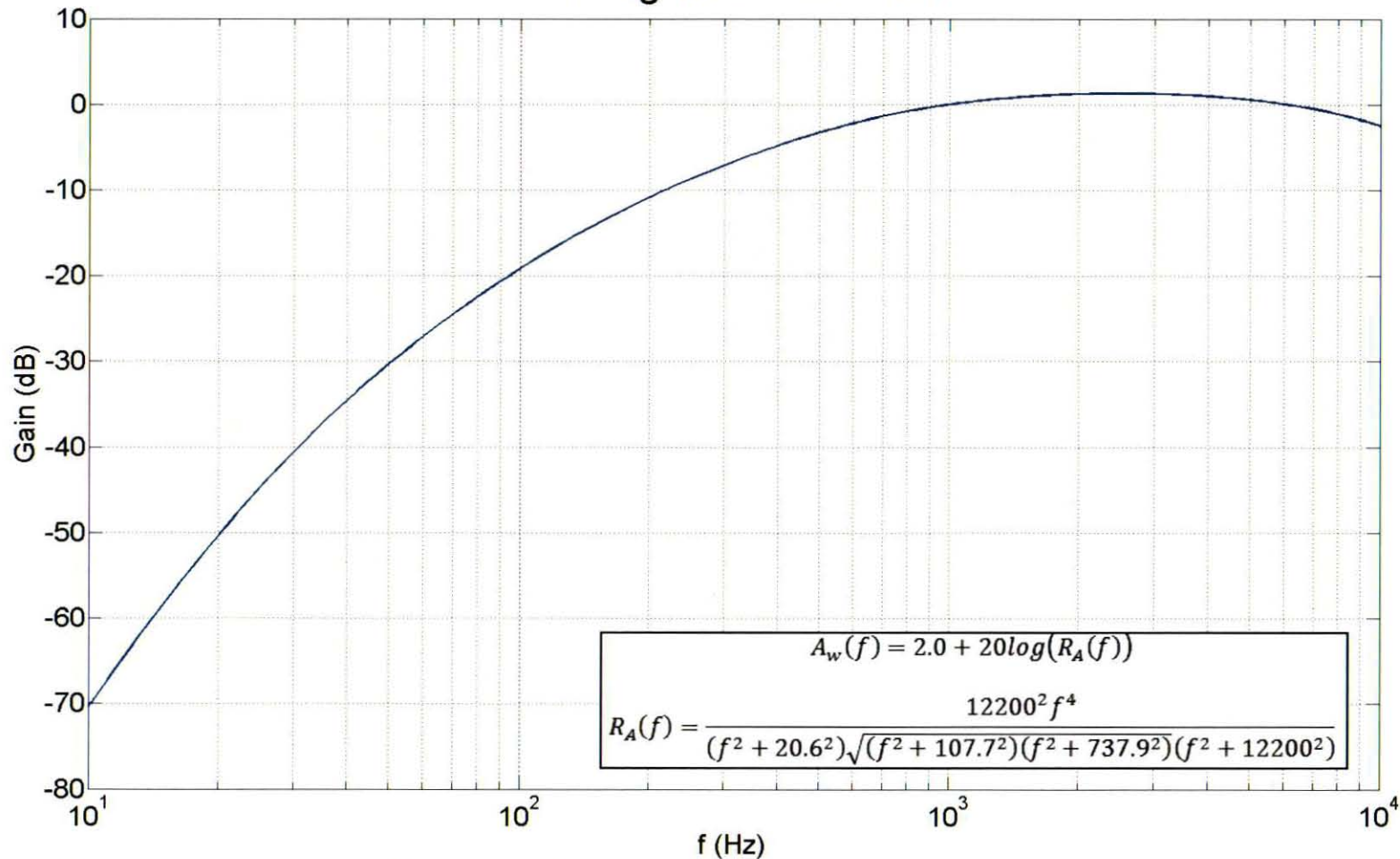
$p_o$  is by standard  $2 \times 10^{-5}$  Pa, this is equivalent to the approximate minimum pressure fluctuation detectable by the human ear



*both  $L_w$  and SPL are indicated in dB*

Source of sound	Sound pressure (Pascal)	Sound pressure level (dB re: 20 $\mu$ Pa)
Theoretical limit for undistorted sound at 1 atmosphere environmental pressure	101,325 Pa	194.0937 dB
Krakatoa explosion at 100 miles (160 km) in air	20,000 Pa	180 dB
Simple open-ended thermoacoustic device	12,000 Pa	176 dB
M1 Garand being fired at 1 m	5,000 Pa	168 dB
Jet engine at 30 m	630 Pa	150 dB
Rifle being fired at 1 m	200 Pa	140 dB
Threshold of pain	100 Pa	130 dB
Hearing damage (due to short-term exposure)	20 Pa	approx. 120 dB
Jet at 100 m	6 – 200 Pa	110 – 140 dB
Jack hammer at 1 m	2 Pa	approx. 100 dB
Hearing damage (due to long-term exposure)	$6 \times 10^{-1}$ Pa	approx. 85 dB
Major road at 10 m	$2 \times 10^{-1}$ – $6 \times 10^{-1}$ Pa	80 – 90 dB
Passenger car at 10 m	$2 \times 10^{-2}$ – $2 \times 10^{-1}$ Pa	60 – 80 dB
TV (set at home level) at 1 m	$2 \times 10^{-2}$ Pa	approx. 60 dB
Normal talking at 1 m	$2 \times 10^{-3}$ – $2 \times 10^{-2}$ Pa	40 – 60 dB
Very calm room	$2 \times 10^{-4}$ – $6 \times 10^{-4}$ Pa	20 – 30 dB
Leaves rustling, calm breathing	$6 \times 10^{-5}$ Pa	10 dB
Auditory threshold at 2 kHz	$2 \times 10^{-5}$ Pa	0 dB

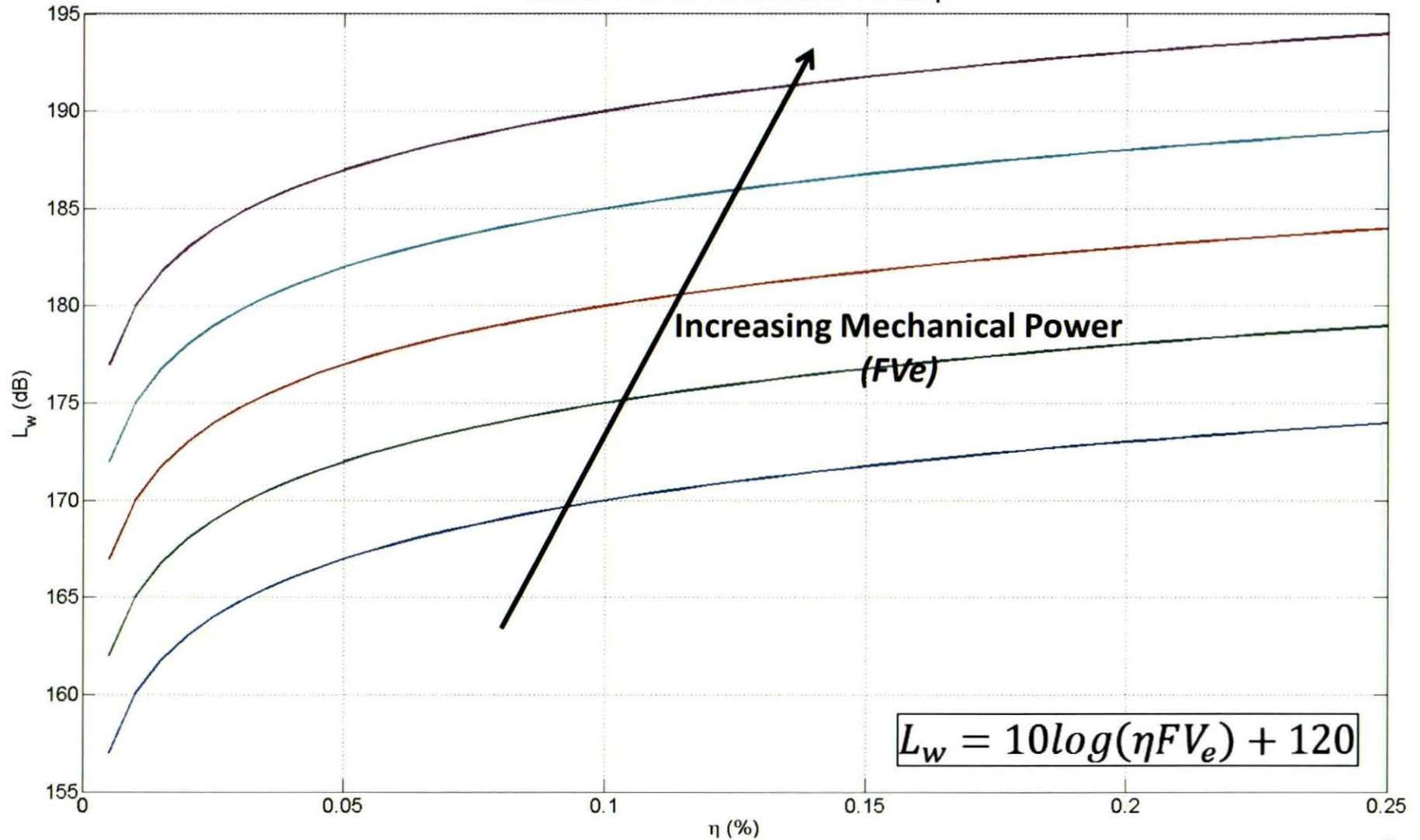
### A-Weighted Correction



- human ear more sensitive at certain frequencies
- low frequency and high frequency sounds perceived to be not as loud as mid-frequency sounds
- ear most sensitive to noise around 2-6 kHz range
- A-weighted curve is the standard for quantifying sounds pressure levels

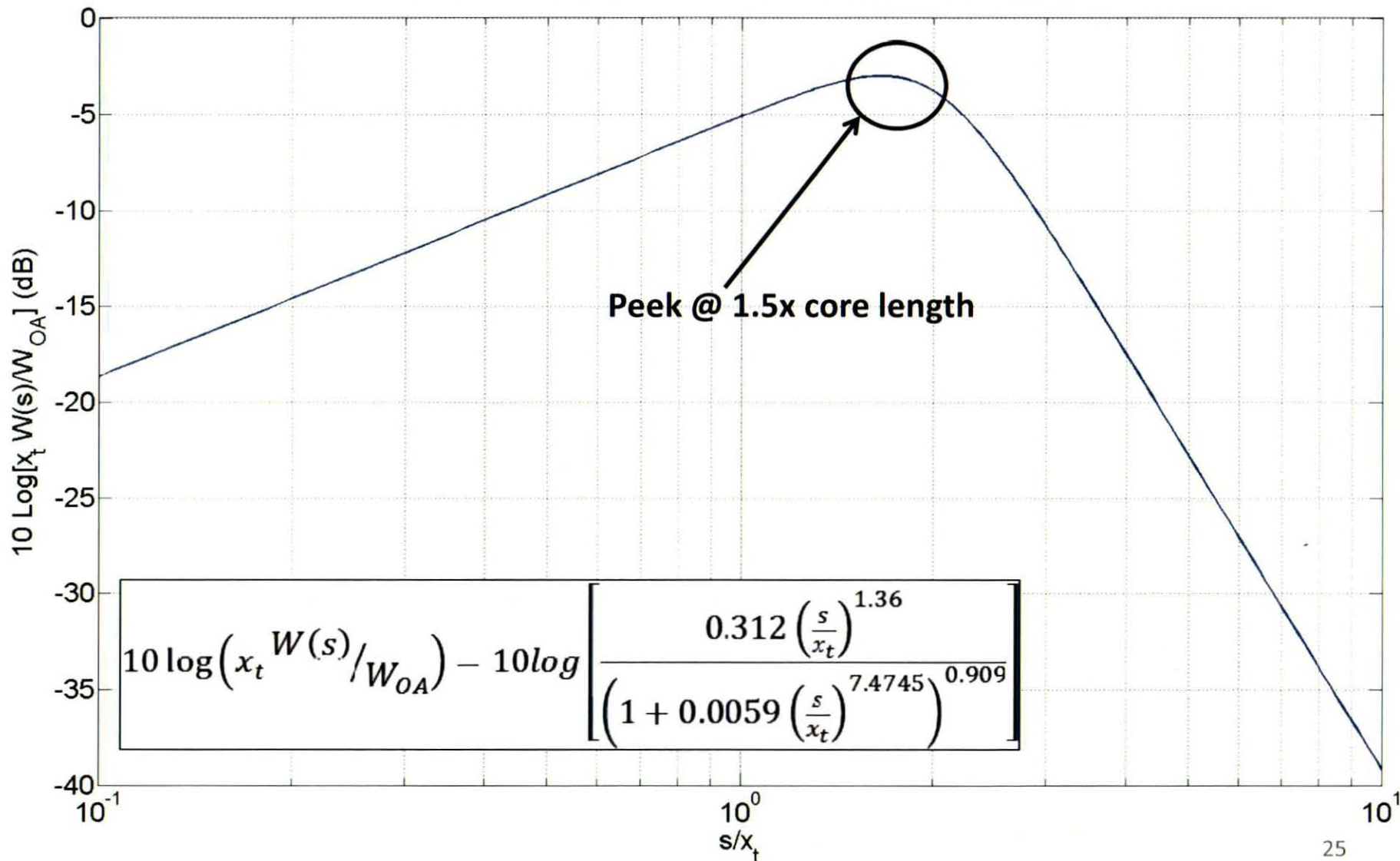
## Aero-Acoustics

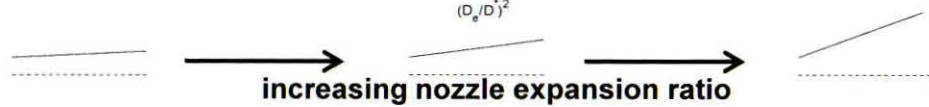
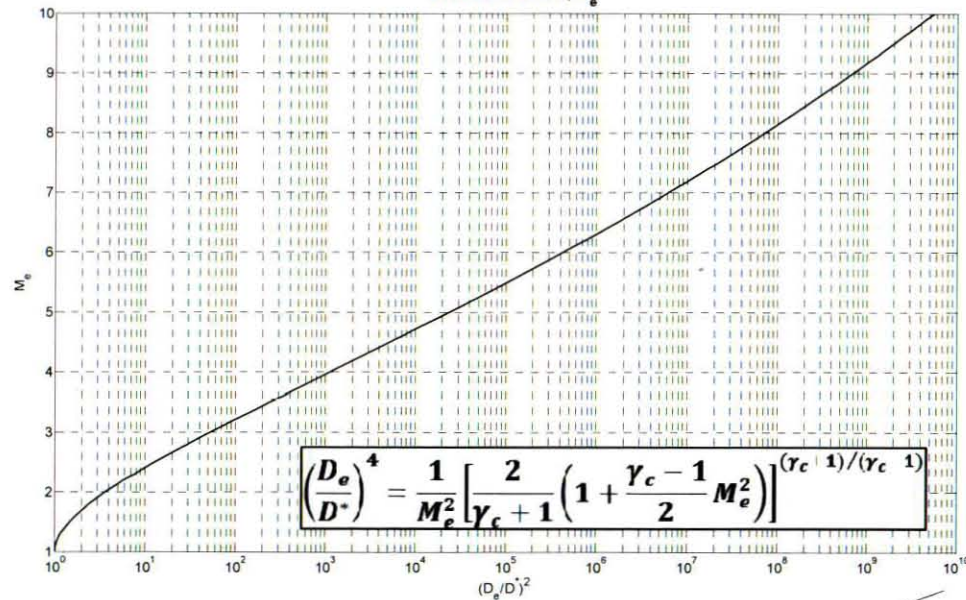
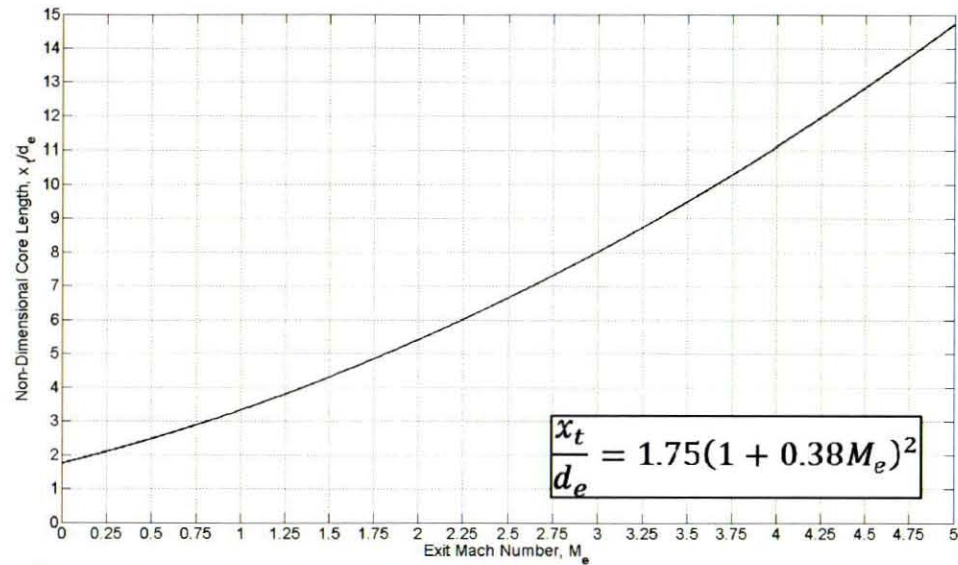
Overall Sound Pressure Level Map



Decreasing Plume Deflection

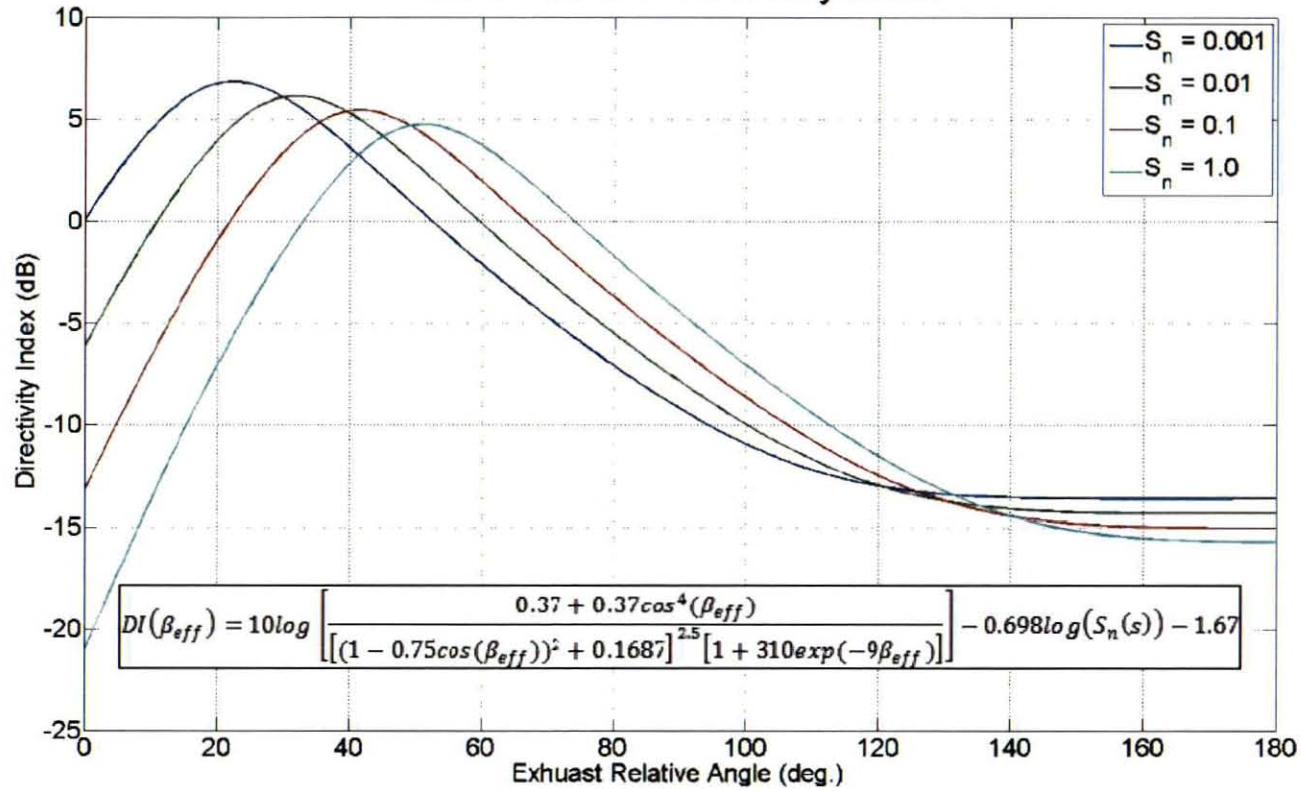
### Normalized Acoustic Power in Plume



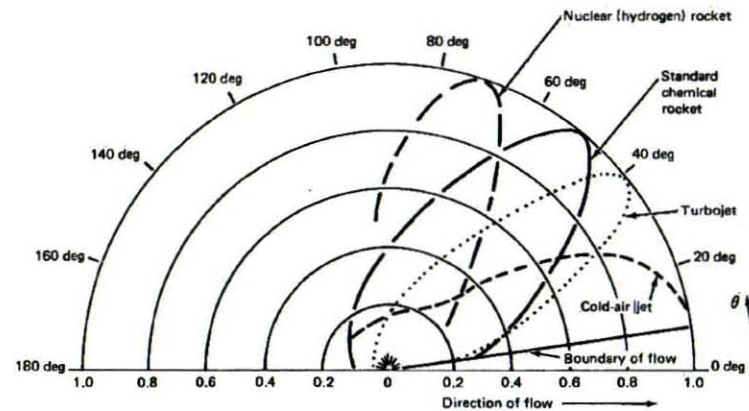




### Plume Source Directivity Index



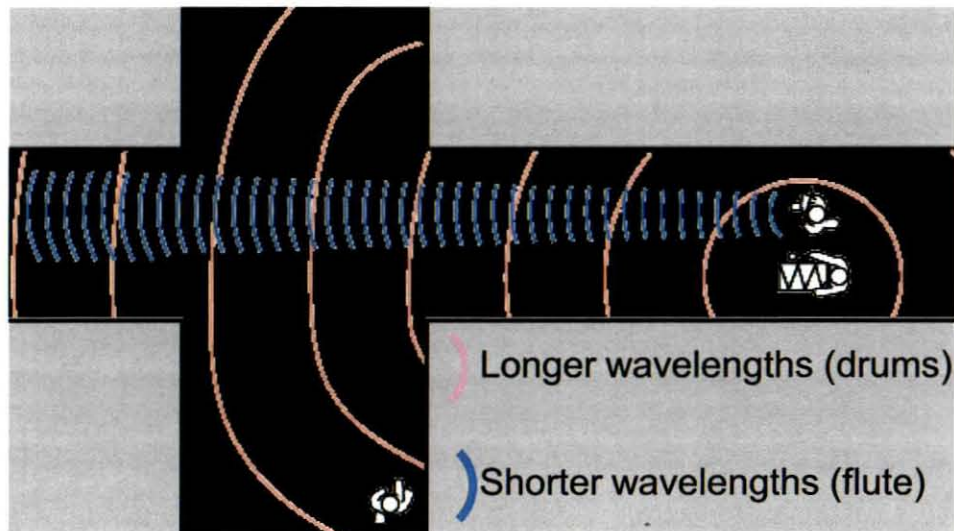
$$DI(\beta_{eff}) = 10 \log \left[ \frac{0.37 + 0.37 \cos^4(\beta_{eff})}{[(1 - 0.75 \cos(\beta_{eff}))^2 + 0.1687]^{2.5} [1 + 310 \exp(-9\beta_{eff})]} \right] - 0.698 \log(S_n(s)) - 1.67$$



## Acoustic Diffraction

# Diffraction Overview

- Bending or spreading of waves around obstacle
  - larger wavelengths will bend around smaller objects or barriers, but not vice versa
- Smaller wavelengths will not diffract around smaller barriers as effectively
  - result known as 'shadow zone' where the sound is quieter than elsewhere around object
- Same conclusion can be made for long wavelengths/longer barriers, which result in a 'shadow zone' due to reflection
- Result of diffraction is reflection, which can affect incident wave (enhance sound intensity levels on surface)

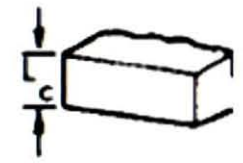
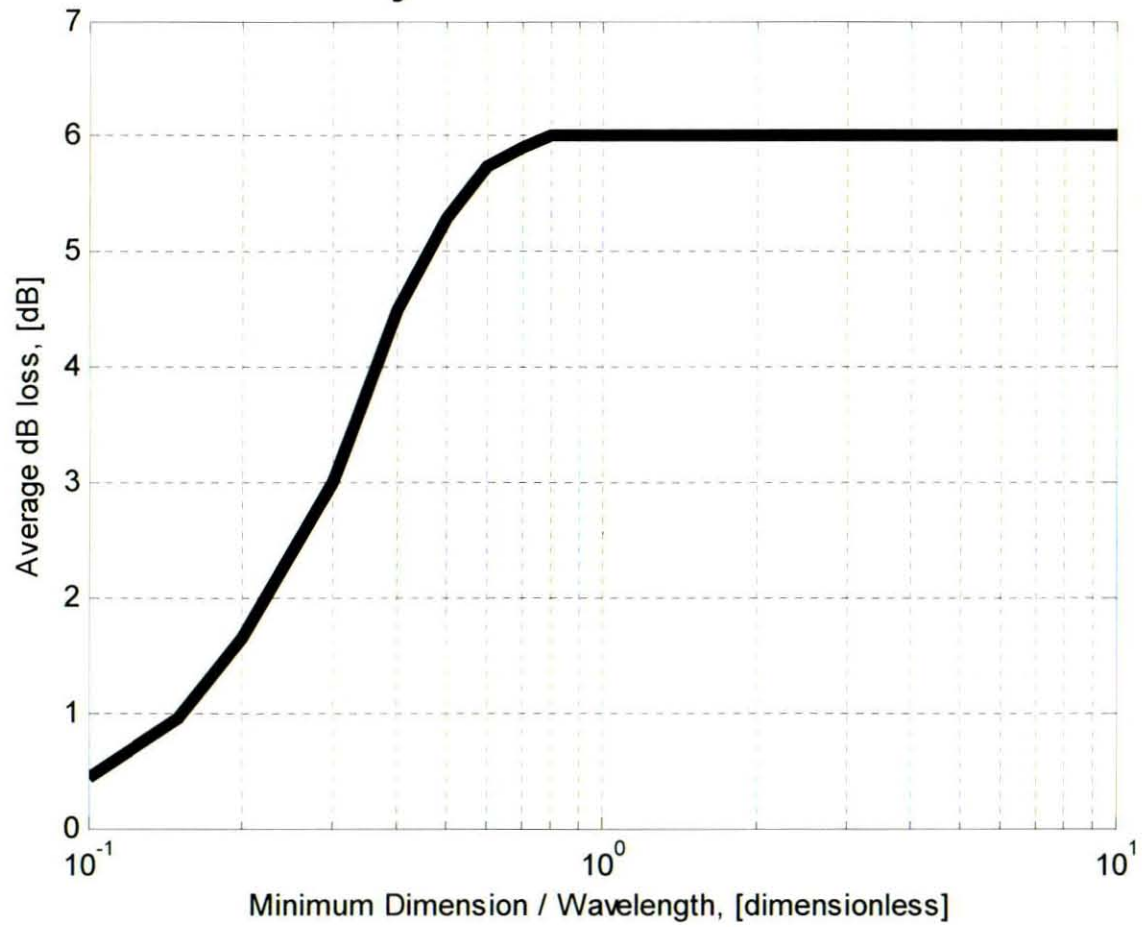


*Total Pressure = Incident Pressure + Pressure Reflected*

$$P_{\text{TOT}} = P_i + P_r$$

# Diffraction Analysis

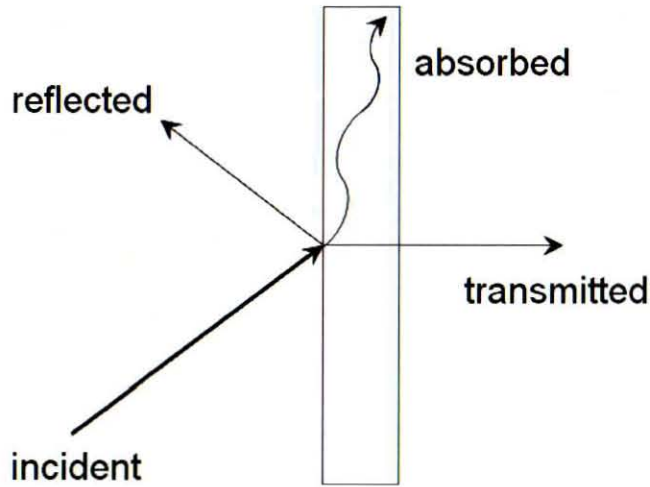
## Wyle dB Loss Model



**NOTE:** Wyle model is average diffraction correction to be applied; if the value of  $L_c / \lambda$  is greater than 10, the dB gain is assumed to be 6 dB.

## Acoustic Transmission

# EFFECTS OF ACOUSTIC LOADS ON STRUCTURES



Sound can either be reflected, absorbed, or transmitted through a wall

ACOUSTIC ABSORPTION COEFFICIENTS						
<b>MATERIALS</b>	<b>125 HZ</b>	<b>250 HZ</b>	<b>500 HZ</b>	<b>1000 HZ</b>	<b>2000 HZ</b>	<b>4000 HZ</b>
<i>5" Thick Fiberglass</i>	0.50	0.97	0.99	0.99	0.97	0.93
<i>Carpet on Concrete</i>	0.11	0.14	0.24	0.40	0.50	0.60
<i>Heavy Window Glass</i>	0.18	0.06	0.04	0.03	0.02	0.02
<i>Marble Tile</i>	0.01	0.01	0.01	0.01	0.02	0.02

# SOUND TRANSMISSION LOSS

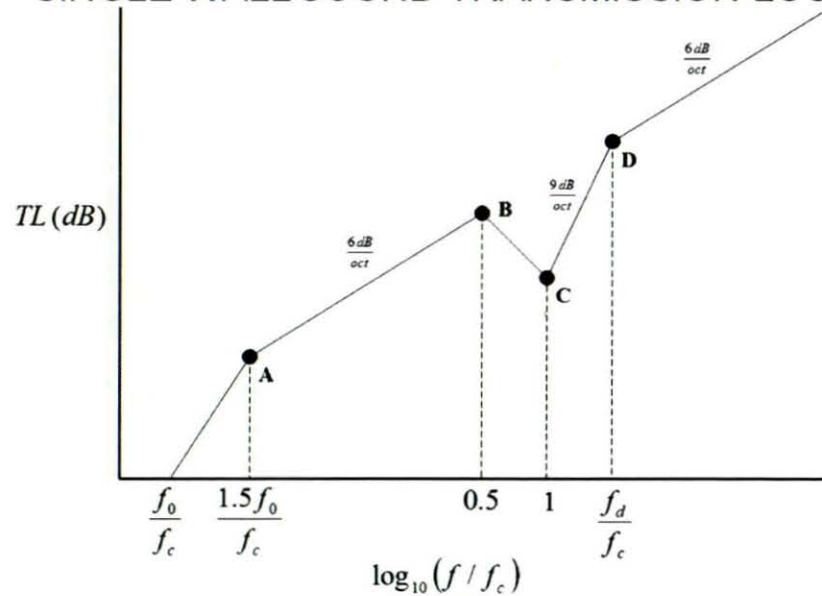
- Transmission loss represents acoustic resistance of structure
- Allows you to quantify the drop in sound through a wall



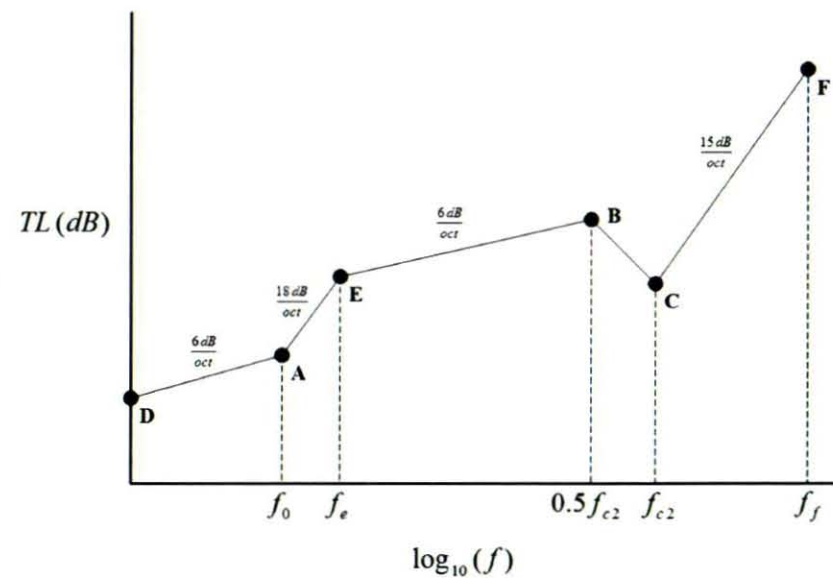
$$SPL_2 = SPL_1 - TL + 10 \log_{10} \left( \frac{A(1 - \bar{\alpha})}{S\bar{\alpha}} \right)$$

$$TL = -10 \log_{10}(\tau)$$

SINGLE WALL SOUND TRANSMISSION LOSS



DOUBLE WALL SOUND TRANSMISSION LOSS



## References



- 1 Eldred, K.M.: Acoustic Loads Generated by the Propulsion System. NASA SP-8072, June 1971.
- 2 29 CFR 1910.95, Occupational Noise Exposure.  
www.osha.gov/pls/oshaweb/owadisp.show\_document?p\_table=standards&p\_id=9735
- 3 Crocker, M.J.: Handbook of Acoustics. Auburn University, 1998.
- 4 Sutherland, L.C.: Sonic and Vibration Environments for Ground Facilities - A Design Manual. WR 68-2, March 1968.
- 5 Anderson, J.D.: Modern Compressible Flow. 3rd Edition, 2003.
- 6 Blitz, J.; Sc., M.; and Inst.P., A.: Elements of Acoustics. Brunel College, 1964.
- 7 Laney, R.C.: Environment Assessment of Vehicle Assembly Building During Accidental Ignition/Burning of Solid Rocket Motor Segments. TWR-11389-1, October 1978.
- 8 Ben-Dor, G.; Igra, O.; and Elperin, T.: Handbook of Shock Waves. Volume 2, 2001.
- 9 Sarafin, T. P.: Spacecraft Structures and Mechanisms: From Concept to Launch. 2003.
- 10 Hill, P.; Peterson, C.: Mechanics and Thermodynamics of Propulsion. 2nd Edition, 1992.
- 11 Barron, R. F.: Industrial Noise Control and Acoustics. 2003.
- 12 Bies, D. A.; Hansen C.: Engineering Noise Control: Theory and Practice. 3rd Edition, 2003.
- 13 Haynes, J., Kenny, R.: Modifications to the NASA SP-8072 Distributed Source Method II for Ares-I Lift-Off Environment Predictions. AIAA-2009-3160. May 2009.